Scientific Voyage
Vol. 1, No. 4,
Page 1-9 (2020)

SCIENTIFIC VOYAGE
ISSN: 2395-5546

GCECT
Publication
Oct.-Dec.

Slowly evolving noncommutative-geometry wormholes

Peter K.F. Kuhfittig[1]
Department of Mathematics, Milwaukee School of Engineering, Milwaukee, Wisconsin 53202-3109, USA

Abstract: This paper discusses noncommutative-geometry wormholes in the context of a cosmological model due to Sung-Won Kim. An ansatz suggested by the Friedmann-Lemaitre-Robertson-Walker (FLRW) model leads to the assumption that the matter content can be divided into two parts, a cosmological part depending only on time and a wormhole part depending only on space. These assumptions are sufficient for deriving a complete zero-tidal force wormhole solution. The wormhole is evolving due to the scale factor in the FLRW model; it is restricted, however, to the curvature parameters $k = 0$ and $k = -1$. Unlike previous models, the noncommutative-geometry background affects both the wormhole part and the cosmological part of the solution.

Keywords: noncommutative geometry; wormholes; FLRW model

1 Introduction

Wormholes are handles or tunnels in spacetime connecting widely separated regions of our Universe or different universes altogether. While there had been some forerunners, macroscopic traversable wormholes were first discussed in detail by Morris and Thorne [1] in 1988. A few years later, Sung-Won Kim [2] proposed the possible existence of an evolving wormhole in the context of the Friedmann-Lemaitre-Robertson-Walker (FLRW) cosmological model by assuming that the matter content can be divided into two parts, the cosmological part that depends on time only and the wormhole part that depends on space only. The discussion was later expanded by Cataldo et al. [3].

The purpose of this paper is to study the relationship between wormholes inspired by noncommutative geometry and the Kim model. The noncommutative-geometry background simultaneously affects both the wormhole construction and the cosmological part of the solution. This result differs significantly from the outcomes in Refs. [2] and [3]. Regarding the strategy, Ref. [1] concentrates mainly on the wormhole geometry by specifying the metric coefficients. This strategy requires a search for matter or fields that can produce the energy-momentum tensor needed to sustain the wormhole. Here it needs to be emphasized that we are able to satisfy the geometric requirements from the physical properties. The result is an evolving zero-tidal force wormhole solution; it is restricted to the curvature parameters $k = 0$ and $k = -1$, corresponding to an open Universe.

Viewed from a broader perspective, it has already been shown that noncommutative geometry, which is an offshoot of string theory, can account for the flat galactic rotation curves [4,5], but under certain conditions, noncommutative geometry can also support traversable wormholes [6–11].

1E-mail: kuhfitti@msoe.edu

This paper is organized as follows: Sec. 2 briefly recalls the structure of wormholes and the basic features of noncommutative geometry. Sec. 3 continues with the Sung-Won Kim model. Here the discussion is necessarily more detailed, partly in the interest of completeness, but mainly to allow the inclusion of a more general form of the Einstein field equations. These are subsequently used in Sec. 6 to obtain a wormhole solution that does not depend on the separation of the matter content. In Sec. 4 we derive a wormhole solution from the noncommutative-geometry background, followed by a discussion of the null energy condition in Sec. 5. Sec. 7 features a comparison to an earlier solution. In Sec. 8, we conclude.

2 Wormhole structure and noncommutative geometry

Morris and Thorne [1] proposed the following static and spherically symmetric line element for a wormhole spacetime:

$$ds^2 = -e^{2\Phi(r)}dt^2 + \frac{dr^2}{1-b(r)/r} + r^2(d\theta^2 + \sin^2\theta\, d\phi^2), \tag{1}$$

using units in which $c = G = 1$. Here $b = b(r)$ is called the *shape function* and $\Phi = \Phi(r)$ is called the *redshift function*, which must be everywhere finite to avoid an event horizon. For the shape function we must have $b(r_0) = r_0$, where $r = r_0$ is the radius of the *throat* of the wormhole. The wormhole spacetime should be asymptotically flat, i.e., $\lim_{r\to\infty}\Phi(r) = 0$ and $\lim_{r\to\infty}b(r)/r = 0$. An important requirement is the *flare-out condition* at the throat: $b'(r_0) < 1$, while $b(r) < r$ near the throat. The flare-out condition can only be met by violating the null energy condition (NEC), which states that

$$T_{\alpha\beta}k^\alpha k^\beta \geq 0, \tag{2}$$

for all null vectors k^α, where $T_{\alpha\beta}$ is the energy-momentum tensor. Matter that violates the NEC is called "exotic" in Ref. [1]. In particular, for the outgoing null vector $(1, 1, 0, 0)$, the violation has the form

$$T_{\alpha\beta}k^\alpha k^\beta = \rho + P^r < 0. \tag{3}$$

Here $T^t{}_t = -\rho$ is the energy density, $T^r{}_r = P^r$ is the radial pressure, and $T^\theta{}_\theta = T^\phi{}_\phi = P^t$ is the lateral pressure.

Returning now to the noncommutative-geometry background mentioned earlier, we need to recall that, as an offshoot of string theory, noncommutative geometry replaces point-like particles by smeared objects. (For a detailed discussion, see Refs. [12–14].) As a result, spacetime can be encoded in the commutator $[\mathbf{x}^\mu, \mathbf{x}^\nu] = i\theta^{\mu\nu}$, where $\theta^{\mu\nu}$ is an antisymmetric matrix that determines the fundamental cell discretization of spacetime in the same way that Planck's constant discretizes phase space [13]. An interesting and effective way to model the smearing effect, discussed in Refs. [9,15,16], is to assume that the energy density of the static, spherically symmetric, smeared, and particle-like gravitational source is given by

$$\rho(r) = \frac{\mu\sqrt{\beta}}{\pi^2(r^2+\beta)^2}, \tag{4}$$

which can be interpreted to mean that the gravitational source causes the mass μ of a particle to be diffused throughout the region of linear dimension $\sqrt{\beta}$ due to the uncertainty; so $\sqrt{\beta}$ has units of length. (Ref. [13] uses a Gaussian distribution instead of Eq. (4) to represent ρ.) Eq. (4) leads to the mass distribution

$$\int_0^r 4\pi (r')^2 \rho(r') dr' = \frac{2M\sqrt{\beta}}{\pi}\left(\frac{1}{\sqrt{\beta}}\tan^{-1}\frac{r}{\sqrt{\beta}} - \frac{r}{r^2+\beta}\right), \tag{5}$$

where M is now the total mass of the source.

According to Ref. [13], noncommutative geometry is one of the basic properties of spacetime that does not depend on particular features such as curvature. Moreover, since the noncommutative effects can be implemented by modifying only the energy-momentum tensor, there is no need to change the Einstein tensor in the field equations. As a result, the length scales need not be microscopic.

3 The Sung-Won Kim model

The Sung-Won Kim cosmological model with a traversable wormhole is given by [2]

$$ds^2 = -e^{2\Phi(r)}dt^2 + [R(t)]^2\left[\frac{dr^2}{1-kr^2-b(r)/r} + r^2(d\theta^2 + \sin^2\theta\, d\phi^2)\right], \tag{6}$$

where $R(t)$ is the scale factor of the Universe and k is the sign of the curvature of spacetime, i.e., $k = +1$, 0, or -1. (So while $b = b(r)$ is still the shape function, it is subject to conditions that are different from those of a Morris-Thorne wormhole.) The Einstein field equations in Ref. [2] are based on Eq. (6), but it is subsequently assumed that $\Phi(r) \equiv 0$ to be consistent with the FLRW model.

The discussion of the Sung-Won Kim model is continued and elaborated on in Ref. [3]. Unfortunately, the field equations in Refs. [2] and [3] do not agree and need to be rederived. Here we follow Ref. [2] and base the calculations on line element (6). The results are

$$8\pi\rho(r,t) = 3\left(\frac{\dot{R}}{R}\right)^2 e^{-2\Phi(r)} + \frac{3k}{R^2} + \frac{b'(r)}{R^2r^2}, \tag{7}$$

$$8\pi P^r(r,t) = -2\frac{\ddot{R}}{R}e^{-2\Phi(r)} - \left(\frac{\dot{R}}{R}\right)^2 e^{-2\Phi(r)} - \frac{k}{R^2} - \frac{b(r)}{R^2r^3} + \frac{2}{R^2r}\Phi'(r)\left(1-kr^2-\frac{b(r)}{r}\right), \tag{8}$$

$$\begin{aligned}8\pi P^t(r,t) = &-2\frac{\ddot{R}}{R}e^{-2\Phi(r)} - \left(\frac{\dot{R}}{R}\right)^2 e^{-2\Phi(r)} - \frac{k}{R^2} + \frac{b(r)-rb'(r)}{2R^2r^3}\\ &+\frac{1}{R^2}\left[(\Phi'(r))^2\left(1-kr^2-\frac{b(r)}{r}\right) + \Phi''(r)\left(1-kr^2-\frac{b(r)}{r}\right)\right.\\ &\left.-\frac{1}{2}\Phi'(r)\left(2kr+\frac{rb'(r)-b(r)}{r^2}\right)\right] + \frac{1}{R^2r}\Phi'(r)\left(1-kr^2-\frac{b(r)}{r}\right),\end{aligned} \tag{9}$$

$$8\pi T_{01} = \frac{\dot{R}}{R^2} e^{-\Phi(r)} \Phi'(r) \left(1 - kr^2 - \frac{b(r)}{r}\right)^{1/2}, \tag{10}$$

where T_{01} is the outward energy flow. (The prime and overdots denote the derivatives with respect to r and t, respectively.)

If $\Phi(r) \equiv 0$, the results agree with those in Ref. [3] (omitting Λ, the cosmological constant). For convenience, these will now be restated:

$$8\pi\rho(r,t) = 3\left(\frac{\dot{R}}{R}\right)^2 + \frac{3k}{R^2} + \frac{b'}{R^2 r^2}, \tag{11}$$

$$8\pi P^r(r,t) = -2\frac{\ddot{R}}{R} - \left(\frac{\dot{R}}{R}\right)^2 - \frac{k}{R^2} - \frac{b}{R^2 r^3}, \tag{12}$$

$$8\pi P^t(r,t) = -2\frac{\ddot{R}}{R} - \left(\frac{\dot{R}}{R}\right)^2 - \frac{k}{R^2} + \frac{b - rb'}{2R^2 r^3}. \tag{13}$$

The next step depends on a key insight, due to Sung-Won Kim [2], that allows the separation of the Einstein field equations into two parts, namely, the following *ansatz* for the matter parts:

$$R^2(t)\rho(r,t) = R^2(t)\rho_c(t) + \rho_w(r), \tag{14}$$

$$R^2(t)P^r(r,t) = R^2(t)P_c(t) + P_w^r(r), \tag{15}$$

$$R^2(t)P^t(r,t) = R^2(t)P_c(t) + P_w^t(r). \tag{16}$$

The subscripts c and w refer, respectively, to the cosmological and wormhole parts. So P_c necessarily represents the isotropic pressure.

The ansatz now allows us to separate Eqs. (11)-(13) into two parts, the left side being a function of t and the right side a function of r, also carried out in Ref. [3]:

$$R^2\left[8\pi\rho_c - 3\left(\frac{\dot{R}}{R}\right)^2 - \frac{3k}{R^2}\right] = \frac{b'}{r^2} - 8\pi\rho_w = l, \tag{17}$$

$$R^2\left[8\pi P_c + 2\frac{\ddot{R}}{R} + \left(\frac{\dot{R}}{R}\right)^2 + \frac{k}{R^2}\right] = -\frac{b}{r^3} - 8\pi P_w^r = m, \tag{18}$$

$$R^2\left[8\pi P_c + 2\frac{\ddot{R}}{R} + \left(\frac{\dot{R}}{R}\right)^2 + \frac{k}{R^2}\right] = \frac{b - rb'}{2r^3} - 8\pi P_w^t = m, \tag{19}$$

where l and m are constants. The reason is that a function of t cannot be equal to a function of r for all t and r unless they are equal to some constant. In Eqs. (18) and (19), the constants are the same since the cosmological parts are equal. The constants l and m may be taken as arbitrary.

Returning now to Eqs. (7)-(10), recall that we obtained the more general form of the field equations by using line element (6), as suggested in Ref. [2]. It now becomes apparent, however, that the separation in Eqs. (17)-(19) cannot be carried out by means of Eqs. (14)-(16) unless we assume that $\Phi(r) \equiv 0$, which takes us back to the FLRW model.

4 The noncommutative wormhole

To obtain a wormhole solution, we will consider the special case $l = -3m$, following Ref. [3]. Eqs. (17)-(19) then yield

$$3\left(\frac{\dot{R}}{R}\right)^2 + \frac{3k}{R^2} - \frac{3m}{R^2} = 8\pi\rho_c \tag{20}$$

and

$$-2\frac{\ddot{R}}{R} - \left(\frac{\dot{R}}{R}\right)^2 - \frac{k}{R^2} + \frac{m}{R^2} = 8\pi P_c, \tag{21}$$

for the cosmological part, while the wormhole part is given by

$$\frac{b'}{r^2} - 8\pi\rho_w = -3m, \tag{22}$$

$$-\frac{b}{r^3} - 8\pi P_w^r = m, \tag{23}$$

$$\frac{b - rb'}{2r^3} - 8\pi P_w^t = m. \tag{24}$$

The wormhole solution can be obtained from Eqs. (22)-(24) by making use of Eq. (4). It remains to be seen what restrictions will be placed on the solutions due to the cosmological part and to the necessary violation of the NEC. But for now we have from Eq. (22) and Eq. (4) that

$$b'(r) = 8\pi\frac{\mu\sqrt{\beta}r^2}{\pi^2(r^2+\beta)^2} - 3mr^2. \tag{25}$$

Integrating and using the condition $b(r_0) = r_0$, we obtain

$$\begin{aligned} b(r) = {} & \frac{4M\sqrt{\beta}}{\pi}\left(\frac{1}{\sqrt{\beta}}\tan^{-1}\frac{r}{\sqrt{\beta}} - \frac{r}{r^2+\beta}\right) - mr^3 \\ & -\frac{4M\sqrt{\beta}}{\pi}\left(\frac{1}{\sqrt{\beta}}\tan^{-1}\frac{r_0}{\sqrt{\beta}} - \frac{r_0}{r_0^2+\beta}\right) + mr_0^3 + r_0, \end{aligned} \tag{26}$$

where M is the mass of the wormhole.

It now becomes apparent that the resulting spacetime is not asymptotically flat. The normal procedure is to cut off the wormhole material at some $r = a$ and then join the structure to an external Schwarzschild spacetime. We will see in the next section, however, that the need to violate the NEC ($\rho + P^r < 0$) requires a slight modification of the shape function, resulting in the required asymptotic flatness.

5 Violating the NEC

To check the violation of the NEC ($\rho + P^r < 0$) for the wormhole, we let $R \equiv$ constant and obtain from Eqs. (11) and (12)

$$b - rb' - 2kr^3 > 0. \tag{27}$$

At $r = r_0$, we therefore get

$$r_0 - r_0 \frac{8\pi\mu\sqrt{\beta}r_0^2}{\pi^2(r_0^2+\beta)^2} + 3mr_0^3 - 2kr_0^3 > 0. \tag{28}$$

Since $\sqrt{\beta}$ is extremely small, we actually have

$$r_0 + (3m - 2k)r_0^3 \geq 0. \tag{29}$$

To check this condition, we need to return to Ref. [13] for some additional observations. The relationship between the radial pressure and energy density is given by

$$P^r = -\rho. \tag{30}$$

The reason is that the source is a self-gravitating droplet of anisotropic fluid of density ρ and the radial pressure is needed to prevent the collapse back to the matter point. In addition, the lateral pressure is given by

$$P^t = -\rho - \frac{r}{2}\frac{\partial\rho}{\partial r}. \tag{31}$$

Since the length scales can be macroscopic, we can retain Eq. (30) and then use Eq. (31) to write

$$P^t = -\rho - \frac{r}{2}\frac{\partial\rho}{\partial r} = P^r + \frac{2\mu r^2\sqrt{\beta}}{\pi^2(r^2+\beta)^3} \tag{32}$$

by Eq. (4).

So on larger scales, we have $P^r = P^t$. Since the pressure becomes isotropic, we can assume the equation of state to be $P_c = -\rho_c$. Substituting in Eqs. (20) and (21), we get

$$-2\frac{\ddot{R}}{R} + 2\left(\frac{\dot{R}}{R}\right)^2 + \frac{2k}{R^2} - \frac{2m}{R^2} = 0. \tag{33}$$

This equation can be rewritten as

$$3\frac{\ddot{R}}{R} - 3\left(\frac{\dot{R}}{R}\right)^2 = \frac{3k}{R^2} - \frac{3m}{R^2}. \tag{34}$$

Subtracting the Friedmann equations

$$3\frac{\ddot{R}}{R} = -4\pi(\rho_c + 3P_c)$$

and

$$3\left(\frac{\dot{R}}{R}\right)^2 = 8\pi\rho_c - \frac{3k}{R^2}$$

now yields

$$\frac{3k}{R^2} - \frac{3m}{R^2} = -4\pi(\rho_c + 3P_c) - 8\pi\rho_c + \frac{3k}{R^2}. \tag{35}$$

So if $P_c = -\rho_c$, we obtain

$$m = 0, \tag{36}$$

independently of k.

Applied to Eq. (29), the NEC is violated if $k = 0$ or $k = -1$. These conditions correspond to an open Universe.

To summarize, we employed basic physical principles to derive the following zero-tidal force solution:

$$\Phi(r) \equiv 0 \tag{37}$$

and (since $m = 0$)

$$\begin{aligned} b(r) &= \frac{4M\sqrt{\beta}}{\pi}\left(\frac{1}{\sqrt{\beta}}\tan^{-1}\frac{r}{\sqrt{\beta}} - \frac{r}{r^2+\beta}\right) \\ &-\frac{4M\sqrt{\beta}}{\pi}\left(\frac{1}{\sqrt{\beta}}\tan^{-1}\frac{r_0}{\sqrt{\beta}} - \frac{r_0}{r_0^2+\beta}\right) + r_0. \end{aligned} \tag{38}$$

The slowly evolving wormhole solution is restricted to the values $k = 0$ and $k = -1$ to ensure that the NEC is violated. The wormhole spacetime is asymptotically flat.

6 The special case $k = 0$

For completeness let us briefly consider a wormhole solution that does not depend on the separation of the Einstein field equations. We can combine Eqs. (11) and (12) to obtain

$$8\pi r^3 R^2 \left[\rho(r,t) + P^r(r,t)\right] = 2r^3(\dot{R}^2 - R\ddot{R}) + 2r^3 k + rb'(r) - b(r). \tag{39}$$

If we now let $k = 0$, then Eq. (6) represents an evolving Morris-Thorne wormhole with the usual shape function $b = b(r)$. The NEC is violated at the throat $r = r_0$ for all t whenever

$$8\pi r_0^3 R^2 \left[\rho(r_0,t) - P^r(r_0,t)\right] = 2r_0^3(\dot{R}^2 - R\ddot{R}) + r_0 b'(r_0) - b(r_0) < 0. \tag{40}$$

If the Universe is indeed accelerating, then the term $-R\ddot{R}$ eventually becomes dominant due to the ever-increasing R. So for sufficiently large R, the NEC is violated, thereby fulfilling a key requirement for the existence of wormholes. (Inflating Lorentzian wormholes are discussed in Ref. [17].)

Recalling that the radial tension τ is the negative of P^r, Inequality (40) can be written (since $b(r_0) = r_0$)

$$8\pi r_0^2 R^2 \left[\tau(r_0) - \rho(r_0)\right] = 2r_0^2(-\dot{R}^2 + R\ddot{R}) - b'(r_0) + 1 > 0. \tag{41}$$

If $R(t) \equiv 1$, this reduces to the static Morris-Thorne wormhole; so if $b'(r_0) < 1$, then $\tau(r_0) > \rho(r_0)$, requiring exotic matter. In Inequality (41), however, $\tau(r_0) > \rho(r_0)$ could result from the dominant term $R\ddot{R}$. In that case, the NEC is violated without requiring exotic matter for the construction of the wormhole itself.

7 Comparison to an earlier solution

A wormhole solution inspired by noncommutative geometry had already been considered in Ref. [9]. The Einstein field equation $\rho(r) = b'(r)/(8\pi r^2)$, together with Eq. (4), leads directly to the static solution, Eq. (38). (Here it is understood that $k = 0$, but $R(t)$ could be retained.) Unfortunately, this simple approach leaves the redshift function undetermined. The desirability of zero tidal forces then suggested the assumption $\Phi(r) \equiv 0$ in Ref. [9]. It is shown in Ref. [18], however, that this assumption causes a Morris-Thorne wormhole to be incompatible with the Ford-Roman constraints from quantum field theory. Given the noncommutative-geometry background, rather than the purely classical setting in Ref. [1], this objection does not apply directly.

It is interesting to note that in the present paper, the zero-tidal force solution is built into the Sung-Won Kim model and does not require any additional considerations.

8 Conclusion

Morris-Thorne wormholes typically require a reverse strategy for their theoretical construction: specify the geometric requirements and then manufacture or search the Universe for matter or fields to obtain the required energy-momentum tensor. One of the goals in this paper is to obtain a complete wormhole solution from certain physical principles. To this end, we assume a noncommutative-geometry background, as in previous studies, but we also depend on a cosmological model due to Sung-Won Kim that is based on the FLRW model with a traversable wormhole. The basic assumption is that the matter content can be divided into two parts, a cosmological part that depends only on t and a wormhole part that depends only on the radial coordinate r. The result is a complete zero-tidal force solution; it is restricted, however, to the values $k = 0$ and $k = -1$, corresponding to an open Universe. This conclusion is consistent with the special case $k = 0$ discussed in Sections 6 and 7.

The wormhole is slowly evolving due to the scale factor $R(t)$ and, critically, the noncommutative-geometry background not only produces the wormhole solution, it also affects in a direct manner the cosmological part of the solution. This conclusion differs significantly from those in Refs. [2] and [3].

References

1. M.S. Morris and K.S. Thorne, *Am. J. Phys.* **56** (1988) 395.
2. S.-W. Kim, *Phys. Rev. D* **53** (1996) 6889.
3. M. Cataldo, F. Arostica and S. Bahamonde, *Phys. Rev. D* **88** (2013) 047502.
4. P.K.F. Kuhfittig, *J. Mod. Phys.* **8** (2017) 323.
5. F. Rahaman, P.K.F. Kuhfittig, K. Chakraborty, A.A. Usmani and S. Ray, *Gen. Rel. Grav.* **44** (2012) 905.
6. P.K.F. Kuhfittig and V.D. Gladney, *J. Mod. Phys.* **5** (2014) 1931.
7. P.K.F. Kuhfittig, *Ind. J. Phys.* **92** (2018) 1207.
8. P.K.F. Kuhfittig, *Sci. Voyage* **2** (2016) 1.
9. P.K.F. Kuhfittig, *Int. J. Mod. Phys. D* **24** (2015) 1550023.
10. M. Jamil, F. Rahaman, R. Myrzakulov, P.K.F. Kuhfittig, N. Ahmed and U. Mondal, *J. Korean Phys. Soc.* **65** (2014) 917.

11. F. Farook, P.K.F. Kuhfittig, S. Ray and S. Islam, *Phys. Rev. D* **86** (2012) 106010.
12. A. Smailagic and E. Spallucci, *J. Phys. A* **36** (2003) L-467.
13. P. Nicolini, A. Smailagic and E. Spallucci, *Phys. Lett. B* **632** (2006) 547.
14. P. Nicolini and E. Spallucci, *Class. Quant. Grav.* **27** (2010) 015010.
15. J. Liang and B. Liu, *Europhys. Lett.* **100** (2012) 30001.
16. K. Nozari and S.H. Mehdipour, *Class. Quant. Grav.* **25** (2008) 175015.
17. T.A. Roman, *Phys. Rev. D* **47** (1993) 1370.
18. P.K.F. Kuhfittig, arXiv: 0908.4233 [gr-qc].

Scientific Voyage
Vol. 1, No. 4,
Page 10-23 (2020)

SCIENTIFIC VOYAGE
ISSN: 2395-5546

GCECT
Publication
Oct.-Dec.

Hawking radiation with the dynamical horizon in the K-essence emergent Vaidya spacetime

Bivash Majumder[a1], Goutam Manna[b2] and Mrinal Manna[c3]

[a] *Department of Mathematics, Prabhat Kumar College, Contai, Purba Medinipur 721404, West Bengal, India*
[b] *Department of Physics, Prabhat Kumar College, Contai, Purba Medinipur 721404, West Bengal, India*
[c] *Department of Physics, Ramakrishna Mission Vivekananda Educational and Research Institute, Belur Math, Howrah 711202, West Bengal, India*

Abstract: We study the Hawking radiation with the dynamical horizon in the **K**-essence Vaidya geometry. By considering the **K**-essence action to be of the Dirac-Born-Infeld variety, the physical spacetime to be a general static spherically symmetric black hole, and by restricting the **K**-essence scalar field to be a function solely of the advanced or the retarded time, Manna et. al. have established the connection between the **K**-essence emergent gravity scenario and generalizations of Vaidya spacetime. Based on modified definition of the dynamical horizon by Sawayama, we investigate the Hawking effect in the **K**-essence Vaidya Schwarzschild spacetime. Especially, we investigate the Hawking Radiation in the two ways, by using the dynamical horizon equation and using the tunneling formalism. The results are different from the usual Vaidya spacetime geometry.

Keywords: Emergent gravity; **K**-essence; Vaidya spacetimes

1. Introduction

It is believed that a black hole is formed by the collapse of matter and it radiates the thermal radiation whose temperature is proportional to the surface gravity [1–10]. In [1], it is assumed that the spacetime is to be static or stationary for calculating Hawking Radiation. This assumption will be valid only when the radiated energy is so small compared to the mass energy of the black hole. When the radiation becomes sufficiently large, it can be modified via Einstein equation. In this context, Vaidya [11,12] has solved nonstatic solution of the Einstein's field equations for spheres of fluids radiating energy. The nonstatic analogs of Schwarzschild's interior solution in General Relativity (GR) has been established in [13,14] and the problem of gravitational collapse with radiation has been solved in [15]. The solution has satisfied the physical feature of allowing a positive definite value of the density of collapsing matter, and it gives the total luminosity of the object as observed by a stationary observer at infinity to be zero when the collapsing object approaches to the Schwarzschilds singularity. So, we can say that the Vaidya spacetime [11–15] is a non-stationary Schwarzschild spacetime. Husain [16] and Wang et. al. [17] have developed the generalizations of Vaidya spacetime corresponding

[1] E-mail: bivashmajumder@gmail.com
[2] E-mail: goutammanna.pkc@gmail.com
[3] E-mail: mrinalmanna1997@gmail.com

to the gravitational collapse of a null fluid. Recently, Manna et al. [18,19] have established the **K**-essence generalizations of Vaidya spacetime where time dependence of the metric comes from the kinetic energy (ϕ_v^2) of the **K**-essence scalar field (ϕ). The Hawking radiation [1–10] has been discussed in [20–24] using tunneling mechanism. Also, it was developed by the method of complex path analysis which is used to describe tunnelling processes in semiclassical quantum mechanics in [25,26]. Kerner and Mann [27] have established, in general, that the Hawking temperature is independent of the angular part of the spacetime. In [28–31], they have discussed the Hawking radiation of Vaidya or Vaidya-Bonner spacetime.

The **K**-essence theory [32–38] is a scalar field theory where the kinetic energy of the field dominates over the potential energy of the field. The differences between the relativistic field theories with canonical kinetic terms and the **K**-essence theory with non-canonical kinetic terms are that the non-trivial dynamical solutions of the K-essence equation of motion, which not only spontaneously break Lorentz invariance but also change the metric for the perturbations around these solutions. Thus the perturbations propagate in the so called *emergent or analogue* curved spacetime with the metric. Based on the Dirac-Born-Infeld (DBI) model [39–41], Manna et al. [42–45] have developed the simplest form of **K**-essence emergent gravity metric $\bar{G}_{\mu\nu}$ which is not conformally equivalent to the usual gravitational metric $g_{\mu\nu}$. The theoretical form in the **K**-essence field, the lagrangian is non-canonical and it does not depend explicitly on the field itself. The general form of the Lagrangian for the **K**-essence model is: $L = -V(\phi)F(X)$ where $X = \frac{1}{2}g^{\mu\nu}\nabla_\mu\phi\nabla_\nu\phi$.

Ashtekar and Krishnan have considered the dynamical horizons in their paper [46–51], and derived a new equation that describe how the dynamical horizon radius changes. The definition of dynamical horizon is as follows: *Dynamical Horizon*: A smooth, three-dimensional, space-like submanifold H in a space-time $\mathcal{M}$ is said to be a dynamical horizon if it can be foliated by a family of closed $2-$surfaces such that, on each leaf S, the expansion $\Theta_{(l)}$ of one null normal l^a vanishes and the expansion $\Theta_{(n)}$ of the other null normal n^a is strictly negative. Also, *this definition can be modified as [52]:* A smooth, three-dimensional, spacelike or timelike submanifold H in a space-time is said to be a dynamical horizon if it is foliated by a preferred family of 2-spheres such that, on each leaf S, the expansion $\Theta_{(l)}$ of a null normal l^a vanishes and the expansion $\Theta_{(n)}$ of the other null normal n^a is strictly negative.

Following [48], in the concept of world tubes, if the marginally trapped tubes (MTT) is spacelike,it is called a dynamical horizon (DH). Under some conditions, it provides a quasi-local representation of an evolving black hole. If it is null, it describes a quasi-local description of a black hole in equilibrium and is called an isolated horizon (IH). If the MTT is timelike, causal curves can transverse it in both inward and outward directions, where it does not represent the surface of a black hole in any useful sense, it is called a timelike membrane (TLM).

In this work, we have studied the Hawking radiation with the dynamical horizon in the **K**-essence emergent Vaidya spacetime based on Sawayama [52] by considering dynamical horizon equation [46–49] and tunneling formalism [20–26,28, 29,42–44].

The paper is organized as follows: In section 2, we briefly discuss the **K**-essence emergent geometry and corresponding **K**-essence Vaidya spacetime. We describe the dynamical horizons considering Schwarzschild black hole as a background for the **K**-essence emergent Vaidya spacetime in section 3. In the next section, we have discussed in detail the dynamical horizon equation for the **K**-essence Vaidya Schwarzschild spacetime. Also, we have discussed the corresponding Hawking radiation using dynamical horizon equation and tunneling mechanism. The Last section is our discussion.

2. Brief review of K-essence and K-essence-Vaidya Geometry

The **K**-essence scalar field ϕ minimally coupled to the background gravitational metric $g_{\mu\nu}$ has action [32]-[36]

$$S_k[\phi, g_{\mu\nu}] = \int d^4x\sqrt{-g}L(X,\phi), \tag{1}$$

where $X = \frac{1}{2}g^{\mu\nu}\nabla_\mu\phi\nabla_\nu\phi$ and the energy-momentum tensor is

$$T_{\mu\nu} \equiv \frac{2}{\sqrt{-g}}\frac{\delta S_k}{\delta g^{\mu\nu}} = L_X\nabla_\mu\phi\nabla_\nu\phi - g_{\mu\nu}L, \tag{2}$$

where $L_{\mathrm{X}} = \frac{dL}{dX}$, $L_{XX} = \frac{d^2L}{dX^2}$, $L_\phi = \frac{dL}{d\phi}$ and ∇_μ is the covariant derivative defined with respect to the gravitational metric $g_{\mu\nu}$.

The scalar field equation of motion is

$$-\frac{1}{\sqrt{-g}}\frac{\delta S_k}{\delta\phi} = \tilde{G}^{\mu\nu}\nabla_\mu\nabla_\nu\phi + 2XL_{X\phi} - L_\phi = 0, \tag{3}$$

where

$$\tilde{G}^{\mu\nu} \equiv L_X g^{\mu\nu} + L_{XX}\nabla^\mu\phi\nabla^\nu\phi, \tag{4}$$

and $1 + \frac{2XL_{XX}}{L_X} > 0$.

Using the conformal transformations $G^{\mu\nu} \equiv \frac{c_s}{L_x^2}\tilde{G}^{\mu\nu}$ and $\bar{G}_{\mu\nu} \equiv \frac{c_s}{L_X}G_{\mu\nu}$, with $c_s^2(X,\phi) \equiv (1 + 2X\frac{L_{XX}}{L_X})^{-1}$ we have [42–44]

$$\bar{G}_{\mu\nu} = g_{\mu\nu} - \frac{L_{XX}}{L_X + 2XL_{XX}}\nabla_\mu\phi\nabla_\nu\phi. \tag{5}$$

Here one must always have $L_X \neq 0$ for c_s^2 to be positive definite and only then equations $(1) - (4)$ will be physically meaningful.

If L is not an explicit function of ϕ then the equation of motion (3) reduces to

$$-\frac{1}{\sqrt{-g}}\frac{\delta S_k}{\delta\phi} = \bar{G}^{\mu\nu}\nabla_\mu\nabla_\nu\phi = 0. \tag{6}$$

Note that for non-trivial spacetime configurations of ϕ, the emergent metric $G_{\mu\nu}$ is, in general, not conformally equivalent to $g_{\mu\nu}$. So ϕ has properties different from canonical scalar fields, with the local causal structure also different from those defined with $g_{\mu\nu}$. We consider the DBI type Lagrangian as [42–44, 39–41]

$$L(X,\phi) = 1 - V(\phi)\sqrt{1-2X}, \tag{7}$$

for $V(\phi) = V$ =constant and kinetic energy of $\phi >> V$, i.e. $(\dot{\phi})^2 >> V$. This is a typical for the **K**-essence fields where the kinetic energy dominates over the potential energy. Then $c_s^2(X,\phi) = 1 - 2X$. For scalar fields $\nabla_\mu\phi = \partial_\mu\phi$. Thus (5) becomes

$$\bar{G}_{\mu\nu} = g_{\mu\nu} - \partial_\mu\phi\partial_\nu\phi. \tag{8}$$

The corresponding geodesic equation for the **K**-essence theory in terms of the new Christoffel connections $\bar{\Gamma}$ is [42–44]

$$\frac{d^2x^\alpha}{d\lambda^2} + \bar{\Gamma}^\alpha_{\mu\nu}\frac{dx^\mu}{d\lambda}\frac{dx^\nu}{d\lambda} = 0, \tag{9}$$

where λ is an affine parameter and

$$\begin{aligned}\bar{\Gamma}^\alpha_{\mu\nu} &= \Gamma^\alpha_{\mu\nu} + \Big(1-2X\Big)^{-1/2}\bar{G}^{\alpha\gamma}\Big[\bar{G}_{\mu\gamma}\partial_\nu\Big(1-2X\Big)^{1/2} \\ &+ \bar{G}_{\nu\gamma}\partial_\mu\Big(1-2X\Big)^{1/2} - \bar{G}_{\mu\nu}\partial_\gamma\Big(1-2X\Big)^{1/2}\Big] \\ &= \Gamma^\alpha_{\mu\nu} - \frac{1}{2(1-2X)}\Big[\delta^\alpha_\mu\partial_\nu X + \delta^\alpha_\mu\partial_\nu X\Big].\end{aligned} \tag{10}$$

2.1 **K***-essence-Vaidya Geometry*

Considering a general spherically symmetric static (black hole) Eddington-Finkelstein line element [18]

$$ds^2 = f(r)dv^2 - 2\epsilon dvdr - r^2d\Omega^2, \tag{11}$$

where $d\Omega^2 = d\theta^2 + sin^2\theta d\Phi^2$. When $\epsilon = +1$, the null coordinate v represents the Eddington advanced time (outgoing), while when $\epsilon = -1$, it represents the Eddington retarded time (incoming).

From (8) the emergent spacetime is described by the line element

$$dS^2 = ds^2 - \partial_\mu\phi\partial_\nu\phi dx^\mu dx^\nu. \tag{12}$$

Considering the scalar field $\phi(x) = \phi(v)$, so that the emergent spacetime line element is

$$dS^2 = \Big[f(r) - \phi_v^2\Big]dv^2 - 2\epsilon dvdr - r^2d\Omega^2, \tag{13}$$

where $\phi_v = \frac{\partial\phi}{\partial v}$.

Notice that this assumption on ϕ actually violates local Lorentz invariance, since in general, spherical symmetry would only require that $\phi(x) = \phi(v,r)$. But in the **K**-essence theory, the dynamical solutions are spontaneously break Lorentz invariance. So, in this context, our choice of form of the **K**-essence scalar field is physically permissible.

Now comparing the emergent spacetime (13) with the metric [16,17] of the generalized Vaidya spacetimes corresponding to gravitational collapse of a null fluid (take $\epsilon = +1$)

$$dS_V^2 = \left(1 - \frac{2m(v,r)}{r}\right)dv^2 - 2dvdr - r^2d\Omega^2, \tag{14}$$

where the mass function is

$$m(v.r) = \frac{1}{2}r\Big[1 + \phi_v^2 - f(r)\Big]. \tag{15}$$

These forms (13) or (14) of metrics are satisfying all the required energy conditions [53] (weak, strong, dominant) for generalizations of the **K**-essence emergent spacetime with the Vaidya spacetime provided $\phi_v\phi_{vv} > 0$; $1+\phi_v^2 > f + rf_r$; $2f_r + rf_{rr} > 0$ which have established by Manna et al. [18].

3. Dynamical horizons

Following Ashtekar and Krishnan [47] and Sawayama [52], we can discuss behavior of the dynamical horizon of the **K**-essence emergent Vaidya spacetime. The generalized Vaidya spacetime (13) or (14) in the presence of kinetic energy of the **K**-essence scalar field ϕ_v^2 can be written as

$$dS^2 = F(v,r)dv^2 - 2dvdr - r^2 d\Omega^2, \tag{16}$$

where v^a is a null vector.

Following Sawayama [52], we can define

$$a = \frac{dr}{dr^*}, \tag{17}$$

where r^* is tortoise coordinate defined as $v = t + r^*$.

There are two null vectors,

$$l^a = \begin{bmatrix} l^t \\ l^{r^*} \\ l^\theta \\ l^\Phi \end{bmatrix} = \begin{bmatrix} a^{-1} \\ -a^{-1} \\ 0 \\ 0 \end{bmatrix}, \tag{18}$$

corresponding to the null vector v^a , and the other is

$$n^a = \begin{bmatrix} n^t \\ n^{r^*} \\ n^\theta \\ n^\Phi \end{bmatrix} = \begin{bmatrix} a^{-1} \\ \frac{F}{F-2a}a^{-1} \\ 0 \\ 0 \end{bmatrix}. \tag{19}$$

The expansions $\Theta_{(l)}$ and $\Theta_{(n)}$ of the two null vectors l^a and n^a are [52]

$$\Theta_{(l)} = \frac{1}{r}(2F - a), \tag{20}$$

and

$$\Theta_{(n)} = \frac{1}{ar}\left(\frac{-2F^2 + aF - 2a^2}{-F + 2a}\right). \tag{21}$$

We can see that as $\Theta_{(l)} = 0 \Rightarrow 2F - a = 0$, and the other null expansion $\Theta_{(n)}$ is strictly negative which are the required conditions for the dynamical horizon [46, 47, 52]. So the horizons of our case are dynamical. Note that, based on Ashtekar et al. [46–50], Manna et al. [18] also have established the possibility of the dynamical horizon for the **K**-essence emergent Vaidya spacetime.

3.1 Schwarzschild black hole as background

In this case $f(r) = 1 - \frac{2M}{r}$, then (16) become

$$dS^2 = \Big(1 - \frac{2M}{r} - \phi_v^2\Big)dv^2 - 2dvdr - r^2 d\Omega^2, \tag{22}$$

with

$$F = \Big(1 - \frac{2M}{r} - \phi_v^2\Big) \equiv \Big(1 - \frac{2m(v,r)}{r}\Big), \tag{23}$$

and the mass function become

$$m(v,r) = M + \frac{r}{2}\phi_v^2, \tag{24}$$

where the tortoise coordinate

$$r^* = \frac{1}{N}\Big[r + B\ ln(r-B)\Big], \tag{25}$$

where $N \equiv N(v) = (1-\phi_v^2)$, $B = 2M'(v) = \frac{2M}{N}$ with $M'(v) = \frac{M}{1-\phi_v^2}$.

Note that in the above spacetime (22) always $\phi_v^2 < 1$. If $\phi_v^2 > 1$, the signature of this spacetime will be ill-defined. Also the condition $\phi_v^2 \neq 0$ holds good instead of $\phi_v^2 = 0$, which leads to non-applicability of the **K**-essence theory.

Now differentiating the above equation (25) with respect to r^* we get

$$\begin{aligned} a = F\Big[1 - \frac{1}{N}\Big(\frac{dB}{dv}\ ln(r-B) - \frac{B}{r-B}\frac{dB}{dv}\Big) \\ + \frac{1}{N^2}\Big(r + B\ ln(r-B)\frac{dN}{dv}\Big)\Big]. \end{aligned} \tag{26}$$

Now we solve $\Theta_{(l)} = 0$, to determine the dynamical horizon radius as

$$\begin{aligned} 2F - a = 2F - F\Big[1 - \frac{1}{N}\Big(\frac{dB}{dv}\ ln(r-B) - \frac{B}{r-B}\frac{dB}{dv}\Big) \\ + \frac{1}{N^2}\Big(r + B\ ln(r-B)\frac{dN}{dv}\Big)\Big] = 0. \end{aligned} \tag{27}$$

From the above equation we have two solutions at $r = r_D$ one is $F = 0$, i.e.,

$$r_D = 2M'(v) = \frac{2M}{1-\phi_v^2}, \tag{28}$$

and another is

$$\begin{aligned} 1 + \frac{d}{dv}\Big[\frac{B}{N}\ ln(r_D - B)\Big] - \frac{r_D}{N^2}\frac{dN}{dv} = 0 \\ \Rightarrow (r_D - B)^B e^{r_D} = e^{-vN}. \end{aligned} \tag{29}$$

The value of r_D can be written in terms of the Wright ω function [55] as

$$r_D = B\Big[1 + \omega(Z)\Big] = \frac{2M}{N}\Big[1 + \omega(Z)\Big], \tag{30}$$

with $Z = -[1 + ln(B) + vC]$, $C = \frac{N^2}{2M} = \frac{(1-\phi_v^2)^2}{2M}$.

The Wright ω function is a single-valued function, defined in terms of the multi-valued Lambert W function [56] as $\omega(Z) = W_{\mathcal{K}(Z)}(e^Z)$ where $\mathcal{K}(Z)(=[\frac{(Im(Z)-\pi)}{2\pi}])$

is the unwinding number of Z. The sign of this unwinding number is such that $ln(e^Z) = Z + 2\pi i\mathcal{K}(Z)$ which is opposite to the sign used in [57]. The algebraic properties [55] of the Wright ω function are

$$\frac{d\omega}{dZ} = \frac{\omega}{1+\omega}, \tag{31}$$

$$\int \omega^n dZ = \begin{cases} \dfrac{\omega^{n+1}-1}{n+1} + \dfrac{\omega^n}{n} & if\ n \neq -1 \\ ln\ \omega - \dfrac{1}{\omega} & if\ n = -1, \end{cases} \tag{32}$$

with the analytic property $Z = \omega + ln\ \omega$.

Here mention that if we consider the usual Vaidya spacetime without **K**-essence scalar field ϕ i.e., $m(v,r) \equiv M(v)$ and $\phi_v^2 = 0$, then from the above equation (29) we can get back to the Sawayama [52] result as

$$r_D = 2M(v) + e^{-v/2M(v)}. \tag{33}$$

4. Dynamical horizon equation and Hawking radiation

From (16), we can construct the Ricci scalar ($\bar{R}$) and the Ricci tensors ($\bar{R}_{\mu\nu}$) of the **K**-essence emergent Vaidya spacetime as

$$\begin{aligned} \bar{R}_{vv} &= \frac{1}{r}\partial_v F - \frac{F}{2}\partial_r^2 F - \frac{F}{r}\partial_r F\ : \\ \bar{R}_{rv} = \bar{R}_{vr} &= \frac{1}{2}\partial_r^2 F + \frac{1}{r}\partial_r F\ :\ \bar{R}_{rr} = 0\ ; \\ \bar{R}_{\theta\theta} &= F + r\partial_r F - 1\ ;\ \bar{R}_{\Phi\Phi} = sin^2\theta \bar{R}_{\theta\theta}\ ; \\ \bar{R} &= -[\partial_r^2 F + \frac{4}{r}\partial_r F + \frac{2}{r^2}(F-1)]. \end{aligned} \tag{34}$$

Using these values of the Ricci scalar and the Ricci tensors (34), we can construct the components of the energy momentum tensor for the **K**-essence emergent Vaidya spacetime through the "emergent" Einstein's equation $\bar{R}_{\mu\nu} - \frac{1}{2}\bar{G}_{\mu\nu}\bar{R} = 8\pi\bar{T}_{\mu\nu}$, taking the gravitational constant $G = 1$, as

$$8\pi\bar{T}_{vv} = \frac{1}{r}\partial_v F + \frac{1}{r}F\partial_r F + \frac{F}{r^2}(F-1), \tag{35}$$

$$8\pi\bar{T}_{vr} = -[\frac{1}{r}\partial_r F + \frac{1}{r^2}(F-1)], \tag{36}$$

$$8\pi\bar{T}_{rr} = 0, \tag{37}$$

$$8\pi\bar{T}_{\theta\theta} = -[\frac{r^2}{2}\partial_r^2 F + r\partial_r F]\ ;\ 8\pi\bar{T}_{\Phi\Phi} = sin^2\theta\bar{T}_{\theta\theta}. \tag{38}$$

Now, *for the Schwarzschild background case (i.e. subcase 3.1)*, the components of the energy-momentum tensors for the spherically symmetric **K**-essence emergent

Schwarzschild Vaidya spacetime (22) are

$$8\pi\bar{T}_{vv} = -\frac{2}{r^2}[\partial_v m + F\partial_r m] = -\left[\frac{2\phi_v\phi_{vv}}{r} + \frac{\phi_v^2}{r^2}(1-\frac{2M}{r}-\phi_v^2)\right], \quad (39)$$

$$8\pi\bar{T}_{vr} = \frac{2}{r^2}\partial_r m = \frac{\phi_v^2}{r^2}$$

$$or\ 8\pi\bar{T}_{vr^*} = \frac{2a}{r^2}\partial_r m = a\frac{\phi_v^2}{r^2}, \quad (40)$$

$$8\pi\bar{T}_{rr} = 8\pi\bar{T}_{r^*r^*} = 0. \quad (41)$$

Following Sawayama [52], we can derive the energy-momentum tensor $\bar{T}_{\hat{t}l}$ for the integration of the dynamical horizon equation exactly stated in [46,47,52] as

$$\frac{1}{2G}(R_2 - R_1) = \int_{\Delta H} T_{ab}\hat{\tau}^a\xi^b_{(R)}d^3V + \frac{1}{16\pi G}\int_{\Delta H} N_R[|\sigma|^2 + 2|\zeta|^2]d^3V, \quad (42)$$

where R_2, R_1 are the radii of the dynamical horizon, T_{ab} is the stress-energy tensor, $|\sigma|^2 = \sigma_{ab}\sigma^{ab}$, $|\zeta|^2 = \zeta_a\zeta^a$, σ_{ab} is the shear, $\zeta^a = \tilde{q}^{ab}\hat{r}^c\nabla_c l_b$, with the two-dimensional metric $\tilde{q}^{ab}$, and $\xi^a_{(R)} = N_R l^a$ with $N_R = |\partial R|$, where R is the radius of the dynamical horizon. This is the dynamical horizon equation that tells us how the horizon radius changes due to the matter flow, shear, and expansion. In the spherically symmetric case, the second term of the right-hand side of the dynamical equation vanishes.

At first, we can write $\bar{T}_{tl}$ in terms of $\bar{T}_{vv}$ and $\bar{T}_{vr^*}$ as

$$\bar{T}_{tl} = \bar{T}_{vv} - \bar{T}_{vr^*} = -\frac{1}{4\pi r^2}\frac{5}{2}\partial_v m = -(\frac{1}{4\pi r^2})\frac{5}{2}r\phi_v\phi_{vv}. \quad (43)$$

Considering $\hat{t}^a$ being the unit vector in the direction of t^a, then we have

$$\bar{T}_{\hat{t}l} = -\frac{1}{4\pi r^2}\frac{5}{2}(\partial_v m)F^{-1}, \quad (44)$$

with F is defined in (23). At the horizon, the expression of $\bar{T}_{\hat{t}l}$ is $\bar{T}_{\hat{t}l}\Big|_{r=r_D} = \frac{1}{4\pi r_D^2}\frac{5r_D}{4}(\partial_v N)F^{-1}$ where we have used $m \equiv m(v,r) = M + \frac{r}{2}(1-N)$.

To evaluate, the dynamical horizon integration (42) in terms of the Wright ω function, at first, we derive some terms as follows:

Using equation (30), we get

$$\frac{dr_D}{dv} = \left[-\frac{2M}{N^2}\Big(1+\omega(Z)\Big) + \frac{2M}{N}\frac{\omega(Z)}{1+\omega(Z)} \times \Big(\frac{1}{N} - \frac{Nv}{M}\Big)\right]\partial_v N - \frac{N\,\omega(Z)}{1+\omega(Z)}. \quad (45)$$

At the horizon, we obtain, from the above equation (45)

$$\partial_v N = \frac{N\,\omega(Z)}{1+\omega(Z)}\Bigg[-\frac{2M}{N^2}\Big(1+\omega(Z)\Big) + \frac{2M}{N}\,\frac{\omega(Z)}{1+\omega(Z)}\,\Big(\frac{1}{N}-\frac{Nv}{M}\Big)\Bigg]^{-1}. \tag{46}$$

and from (30)

$$\frac{dr_D}{dN} = \Big(\frac{N}{\partial_v N}\Big)\frac{\omega(Z)}{1+\omega(Z)}. \tag{47}$$

Now, re-write the equation (23) in terms of Write ω function as

$$F = \frac{N\,\omega(Z)}{1+\omega(Z)}, \tag{48}$$

and from the equation (24)

$$\partial_v m = -\Big(\frac{r_D}{2}\Big)\partial_v N. \tag{49}$$

Changing the order of integration r_D to N in dynamical horizon integration (42), we have

$$\frac{1}{2}\left[\frac{2M}{N}(1+\omega(Z))\right]\Bigg|_{N_1}^{N_2} = \frac{5}{4}\int_{N_1}^{N_2}\frac{2M}{N}(1+\omega(Z))dN, \tag{50}$$

since in the above calculation, the functions $\partial_v N$ and F^{-1} with fixed r_D are used only in the integration.

Now, using the equations (44) to (49) and inserting the above equation (50) in the equation (42) and taking the limit $N_2 \to N_1 = N$, we have

$$-\frac{M}{N^2}\Big(1+\omega(Z)\Big) + \frac{M}{N}\frac{\omega(Z)}{(1+\omega(Z))}\Big(\frac{1}{N}-\frac{Nv}{M}\Big) - \frac{5}{2}\frac{M}{N}\Big(1+\omega(Z)\Big) = 0, \tag{51}$$

which is the dynamical horizon equation for the spherically symmetric **K**-essence emergent Schwarzschild Vaidya spacetime. This dynamical horizon equation in the presence of the kinetic energy of the **K**-essence scalar field is far different from the usual Vaidya dynamical horizon equation [52].

Now *we discuss about the Hawking radiation [1–10]:*
To solve this problem, we consider two ideas, which are (1) to use the dynamical horizon equation (42), and (2) to use the **K**-essence Schwarzschild Vaidya metric (22) using tunneling mechanism [20–26, 28, 29].

4.1 Using the dynamical horizon equation
Considering the result of Candelas [54], for the matter on the dynamical horizon,

which assumes that spacetime is almost static and is valid near the horizon [52], from (22), $r \sim 2m(\equiv \frac{2M}{N})$

$$\bar{T}_{tl} = \frac{-1}{2\pi^2(1-\frac{2m}{r})}\int_0^\infty \frac{w^3 dw}{e^{8\pi m w}-1} = \frac{-1}{2m^4\pi^2 c(1-\frac{2m}{r})}, \quad (52)$$

with $c = 15\times 8^4 = 61440$, where we have used the following value of the integration $\int_0^\infty \frac{w^3 dw}{e^{bw}-1} = \frac{\pi^4}{15b^4}$.

The matter energy of the equation (52) is negative near $r \sim 2m$, which means that in the dynamical horizon equation, the **K**-essence Schwarzschild Vaidya black hole absorbs negative energy, i.e., the black hole radius decreases. Note that, the **K**-essence Schwarzschild Vaidya mass $m(\equiv \frac{M}{1-\phi_v^2})$, at near the horizon, is greater than the Schwarzschild mass as $\phi_v^2 < 1$. Also, the dynamic behavior of the mass function $m(v,r)$ is carried by the kinetic energy (ϕ_v^2) of the **K**-essence scalar field which is defined by the equation (24). Here we use the dynamical horizon equation, since we need only information about the matter near the horizon, without solving the full Einstein equation with the backreaction.

Now following [52], we can get

$$\bar{T}_{\hat{t}l} = \frac{1}{2m^4\pi^2 c(1-\frac{2m}{r})}. \quad (53)$$

Again, by changing the order of integration of the right hand side from r_D to N of the dynamical horizon equation (42)

$$\int_{r_1}^{r_2} 4\pi r_D^2 \bar{T}_{\hat{t}l} dr_D = b\int_{N_1}^{N_2}\Big[\frac{2M}{N}(1+\omega(Z))\Big]^2\frac{(1+\omega(Z))}{(N\omega(Z))}\times \Big[M+\frac{M}{N}(1+\omega(Z))(1-N)\Big]^{-4}\Big(\frac{dr_D}{dN}\Big)dN$$
$$= b\int_{N_1}^{N_2}\Big[\frac{2M}{N}(1+\omega(Z))\Big]^2\times\Big[M+\frac{M}{N}(1+\omega(Z))(1-N)\Big]^{-4}\Big(\frac{1}{\partial_v N}\Big)dN, \quad (54)$$

where $b = \frac{2}{\pi c}$ is a constant. Since in our case, the time dependence of the **K**-essence Schwarzschild Vaidya metric is carrying ϕ_v^2 i.e., $N(=1-\phi_v^2)$.

Now insert this integration (54) into the dynamical horizon equation (42), we obtain

$$\frac{1}{2}\Big[\frac{2M}{N}\Big(1+\omega(Z)\Big)\Big]\Big|_{N_1}^{N_2} = b\int_{N_1}^{N_2}\Big[\frac{2M}{N}\Big(1+\omega(Z)\Big)\Big]^2\times \Big[M+\frac{M}{N}\Big(1+\omega(Z)\Big)(1-N)\Big]^{-4}\Big(\frac{1}{\partial_v N}\Big)dN + \frac{5}{4}\int_{N_1}^{N_2}\frac{2M}{N}\Big(1+\omega(Z)\Big)dN. \quad (55)$$

Now taking the limit $N_2 \to N_1 = N$ and $\omega(Z) \neq 0$, the dynamical horizon equation becomes

$$M^2\left[1+\Big(1-\frac{1}{N}\Big)\Big(1+\omega(Z)\Big)\right]^4 = \frac{4b(1+\omega(Z))^3}{N^3\omega(Z)}\left[\frac{1}{2}-\frac{5(1+\omega(Z))}{4}\times\right.$$
$$\left.\left(-\frac{1+\omega(Z)}{N}+\frac{\omega(Z)}{1+\omega(Z)}\Big(\frac{1}{N}-\frac{Nv}{M}\Big)\right)^{-1}\right]^{-1}. \tag{56}$$

Here we are using the fact that $N \neq 0$ and $M \neq 0$. In this section, our main objective is to find the behavior of the mass of the black hole $m(v,r)$ with v for fixed M as in [52]. To conclude this, we have calculated the equation (56) to find $N(=1-\phi_v^2)$ as a function of z but this equation (56) is a transcendental equation and it cannot solve analytically or numerically since it includes the wright omega function and higher degrees of N. So that this equation (56) fails to find the behavior of the mass of the black hole $m(v,r)$ (for fixed M) through the relation $m(v,r) = M + \frac{r}{2}(1-N)$ at the horizon.

4.2 Using the tunneling formalism

To calculate the Hawking temperature using *tunnelling formalism* [20–26, 28, 29, 42–44], consider a massless particle in a black hole (22) background is described by the Klein-Gordon equation

$$\hbar^2 \left(-\bar{G}\right)^{-1/2} \partial_\mu \left(\bar{G}^{\mu\nu} \left(-\bar{G}\right)^{1/2} \partial\nu\Psi\right), \tag{57}$$

where Ψ can be taken in the form

$$\Psi = exp\left(\frac{i}{\hbar}S + ...\right), \tag{58}$$

to obtain the leading order in $\hbar$ the Hamilton-Jacobi equation is

$$\bar{G}^{\mu\nu}\partial_\mu S \partial_\nu S = 0, \tag{59}$$

considering S is independent of θ and Φ.

Therefore, we have

$$2\partial_v S \partial_r S + \left(1 - \frac{2M}{r} - \phi_v^2\right)\left(\partial_r S\right)^2 = 0 \tag{60}$$

Now, let us choose the action S in the following form [29]

$$S(v,r) = -\int_0^v E(v')dv' + S_0(v,r), \tag{61}$$

so that

$$\partial_v S = -E(v) + \partial_v S_0 \text{ and } \partial_r S = \partial_r S_0.$$

Since S_0 is dependent on v and r, so we can write

$$\frac{dS_0}{dr} = \partial_r S_0 + \frac{dv}{dr}\partial_v S_0 = \partial_r S_0 + \frac{2}{F}\partial_v S_0, \tag{62}$$

where we have used $\frac{dv}{dr} = \frac{2}{F}$, F is defined in equation (23).

Now applying the equations (62) and (62) in equation (60), we get

$$F\frac{dS_0}{dr} = 2E(v), \tag{63}$$

since $\partial_r S_0 \neq 0$.

Therefore, we can obtain the solution of S_0 as

$$\begin{aligned} S_0 = 2E(v)\int\frac{dr}{F} &\equiv 2E(v)\int\frac{dr}{(1-\frac{2M}{r}-\phi_v^2)} \\ = \frac{2E(v)}{N}\int\frac{r\ dr}{r-2M/N} &= 2\pi i\frac{4ME(v)}{N^2}, \end{aligned} \tag{64}$$

with $N = 1-\phi_v^2$.

Here, we have used the Cauchy-integral formula since in the integral, r is analytic inside and on any simple closed contour C which is taken in the positive sense and $\frac{2M}{N}$ is a point interior to C. Therefore, (61) become,

$$S(v,r) = -\int_0^v E(v')dv' + 2\pi i\frac{4ME(v)}{N^2}. \tag{65}$$

So the wave function for the outgoing (and ingoing) massless particle can be read as

$$\Psi_{out}(v,r) = exp\Big[\frac{i}{\hbar}\Big(-\int_0^v E(v')dv' + \pi i\frac{4ME(v)}{N^2}\Big)\Big], \tag{66}$$

$$\Psi_{in}(v,r) = exp\Big[\frac{i}{\hbar}\Big(-\int_0^v E(v')dv' - \pi i\frac{4ME(v)}{N^2}\Big)\Big]. \tag{67}$$

The tunneling rate for the outgoing particle is

$$\Gamma \sim e^{-2ImS} \sim e^{-2\frac{4\pi ME(v)}{N^2}} = e^{-\frac{E(v)}{K_BT}}, \tag{68}$$

where K_B is Boltzman Constant.

Therefore, the Hawking temperature is

$$T_H = \frac{1}{8\pi K_B}\frac{N^2}{M} = \frac{1}{8\pi K_B}\frac{(1-\phi_v^2)^2}{M}. \tag{69}$$

If we consider $\phi_v^2 = 0$ and $m(v,r) = M(v)$, then we can get back the usual Hawking temperature for the Vaidya spacetime [30].

4. Conclusion

Based on Sawayama's [52] modified definition of the dynamical horizon, we have investigated the Hawking radiation in the **K**-essence emergent Vaidya spacetime. Manna et al. [18] have established the connection between the **K**-essence geometry and the Vaidya spacetime, and hence generated the new spacetime namely "the **K**-essence emergent Vaidya spacetime". We evaluate the dynamical horizon equation (51) for the spherically symmetric **K**-essence emergent Schwarzschild Vaidya spacetime which is different from the Sawayama's result, i.e., the usual Vaidya dynamical horizon equation.

From this study of the Hawking radiation using the dynamical horizon equation, we have arrived to the transcendental equation (56) which is far different from the Sawayama's [52] transcendental equation (38) and this equation can not be solved analytically in the presence of the Wright omega function [55] but in future one can find a numerical solution of this equation. So, in this case, we are not able to find that the behavior of the mass of the **K**-essence emergent Schwarzschild Vaidya black hole $m(v,r)$ (for fixed M) at the horizon from the relation $m(v,r) = M + \frac{r}{2}(1-N)$. On the other hand, we have also evaluated the Hawking temperature for the **K**-essence emergent Schwarzschild Vaidya metric (22) using tunneling mechanism. The Hawking temperature is $T_H = \frac{1}{8\pi K_B}\frac{(1-\phi_v^2)^2}{M}$, which is different from the usual Vaidya case.

We hasten to add, two of us (B.M. and G.M.) has coauthored papers [42–45], used the **K**-essence theory as a class of theoretical model of the dark energy. But here we use this theory from a purely gravitational standpoint, rather than the cosmological context of dark energy whose very existence is still not beyond doubt [58,59], based on the latest analysis of data from the Planck consortium [60].

References

1. S. Hawking, *Commun. Math. Phys.* **43** (1975) 199.
2. S. Hawking, *Phys. Rev. Lett.* **26** (1971) 1344.
3. L. Smarr, *Phys. Rev. Lett.* **71** (1973) 30.
4. J. Bardeen, B. Carter and S. Hawking, *Commun. Math. Phys.* **31** (1973) 161.
5. S. Hawking, *Nature* (London) **30** (1974) 248.
6. J. Bekenstein, *Phys. Rev. D* **7** (1973) 2333.
7. J. Bekenstein, *Phys. Rev. D* **9** (1974) 3292.
8. G. Gibbons and S. Hawking, *Phys. Rev. D* **15** (1977) 2738.
9. W.M. Unruh, *Phys. Rev. Lett.* **46** (1981) 1351.
10. S.W. Hawking, G.T. Horowitz and S.F. Ross, *Phys. Rev. D* **51** (1995) 4302.
11. P.C. Vaidya, *Phys. Rev.* **83** (1951) 1.
12. P.C. Vaidya and I.M. Pandya, *Prog. Theo. Phys.* **35** (1966) 1.
13. P.C. Vaidya, *Phys. Rev.* **174** (1968) 5.
14. P.C. Vaidya, *Gen. Rel. Gravit.* **31** (1999) 1.
15. P.C. Vaidya, *Astrophys. J.* **144** (1966) 3.
16. V. Husain, *Phys. Rev. D* **53** (1996) 4.
17. A. Wang and Y. Wu, *Gen. Rel. Gravit.* **31** (1999) 1.
18. G. Manna et. al., *Phys. Rev. D* **101** (2020) 124034.
19. G. Manna, *Eur. Phys. J. C* **80** (2020) 813.
20. M.K. Parikh and F. Wilczek, *Phys. Rev. Lett.* **85** (2000) 5042.
21. P. Mitra, *Phys. Lett. B* **648** (2007) 240.
22. B. Chatterjee, A. Ghosh and P. Mitra, *Phys. Lett. B* **661** (2008) 307.
23. B. Chatterjee and P. Mitra, *Phys. Lett. B* **675** (2009) 240.
24. P. Mitra, Report number: SINP/TNP/96-05, arXiv: 0902.2055.
25. K. Srinivasan and T. Padmanabhan, *Phys. Rev. D* **60** (1999) 024007.
26. S. Shankaranarayanan, T. Padmanabhan and K. Srinivasan, *Class. Quantum Gravit.* **19** (2002) 2671.
27. R. Kerner and R.B. Mann, *Phys. Rev. D* **73** (2006) 104010.
28. Y. Kuroda, *Prog. Theor. Phys.* **71** (1984) 1422.
29. H.M. Siahaan and Triyanta, *Int. J. Mod. Phys.* **A25** (2010) 145.
30. H. Tang et al., *Int. J. Theor. Phys* **57** (2018) 2145.
31. S. Wanglin et al., *Nucl. Phys. B* (Proc. Suppl.), **166** (2007) 270.
32. M. Visser, C. Barcelo and S. Liberati, *Gen. Rel. Gravit.* **34** (2002) 1719.
33. E. Babichev, V. Mukhanov and A. Vikman, *JHEP* **0609** (2006) 061.

34. E. Babichev, M. Mukhanov and A. Vikman, *JHEP* **0802** (2008) 101.
35. A. Vikman, *K-essence: Cosmology, causality and Emergent Geometry*, (Dissertation an der Fakultat fur Physik, Arnold Sommerfeld Center for Theoretical Physics, der Ludwig-Maximilians-Universitat Munchen, Munchen, den 29.08.2007).
36. E. Babichev, M. Mukhanov and A. Vikman, *Looking beyond the Horizon* (WSPC-Proceedings, October 23, 2008).
37. R.J. Scherrer, *Phys. Rev. Lett.* **93** (2004) 011301.
38. L.P. Chimento, *Phys. Rev. D* **69** (2004) 123517.
39. M. Born and L. Infeld, *Proc. Roy. Soc. Lond A* **144** (1934) 425.
40. W. Heisenberg, *Zeit. Phys.* **113** (1939) 61.
41. P.A.M. Dirac, *R. Soc. London Proc. Series A* **268** (1962) 57.
42. D. Gangopadhyay and G. Manna, *Euro. Phys. Lett.* **100** (2012) 49001.
43. G. Manna and D. Gangopadhyay, *Eur. Phys. J. C* **74** (2014) 2811.
44. G. Manna and B. Majumder, *Eur. Phys. J. C* **79** (2019) 553.
45. G. Manna et al., *Eur. Phys. J. Plus* **135** (2020) 107.
46. A. Ashtekar and B. Krishnan, *Phys. Rev. Lett.* **89** (2002) 26.
47. A. Ashtekar and B. Krishnan, *Phys. Rev. D* **68** (2003) 104030.
48. A. Ashtekar and G.J. Galloway, *Adv. Theor. Math. Phys.* **9** (2005) 1.
49. A. Ashtekar and B. Krishnan, *Liv. Rev. Rel.* **7** (2004) 10.
50. S.A. Hayward, *Phys. Rev. D* **49** (1994) 6467.
51. B. Krishnan, *Quasi-local Black Hole Horizons.* In: A. Ashtekar and V. Petkov (eds) Springer Handbook of Spacetime (Springer Handbooks. Springer, Berlin, Heidelberg. $https://doi.org/10.1007/978-3-642-41992-8_25$, 2014).
52. S. Sawayama, *Phys. Rev. D* **73** (2006) 064024.
53. S.W. Hawking and G.F.R. Ellis, *The Large Scale Structure of Spacetime* (Cambridge University Press, Cambridge, 1973).
54. P. Candelas, *Phys. Rev. D* **21** (1980) 2185.
55. R.M. Corless and D.J. Jeffrey, *Artificial Intelligence, Automated Reasoning, and Symbolic Computation* (AISC 2002, Calculemus 2002. Lecture Notes in Computer Science, vol 2385, Springer, Berlin, Heidelberg).
56. R.M. Corless et al., *Adv. in Comput. Math.* **5** (1996) 329.
57. R.M. Corless and D.J. Jeffrey, *Sigsam Bulletin* **30** (1996) 28.
58. J.T. Nielsen, A. Guffanti and S. Sarkar, *Sci. Rep.* **6** (2016) 3559.
59. J. Colin et al., *Astron. Astrophys.* **631** (2019) L13.
60. P.R. Ade et al., Planck Collaboration: Planck 2015 results. XX. Constraints on inflation, *Astron. Astrophys.* (Inflation-driver: September 2017).

Scientific Voyage
Vol. 1, No. 4,
Page 24-27 (2020)

SCIENTIFIC VOYAGE

ISSN: 2395-5546

GCECT
Publication
Oct.-Dec.

Bioremediation of lead and chromium by bacteria isolated from coal mining areas

Rini Roy [a1] and Aditi Nag Chaudhuri [b2]

[a]*Post Graduate Department of Microbiology, Bidhannagar College, Kolkata*
[b]*Post Graduate Department of Microbiology, Lady Brabourne College, Kolkata*

Abstract: The microorganisms present in the soil of coal mining areas are naturally exposed to various heavy metals. Bacterial strain was isolated from soil of the coal mining areas of Raniganj. Metallothioneins (MTs) are a group of low molecular mass, cysteine-rich proteins used in metal homeostasis. The main objective of this study was to isolate and extract MT from the isolated bacterial culture. Induction of MT having molecular weight 14 kD occurs in isolated bacteria upon treatment with heavy metals like lead (Pb) and chromium (Cr) as evidenced from SDS PAGE. The thiol content increased in metal treated cultures when compared to the control sample. FTIR study shows the interaction of Pb (II) and Cr (VI) with cell wall components. The expression of MT was confirmed by Western blot technique. Heavy metal tolerating mechanisms within the isolated bacterial cells may be exhibited in the form of metallothioneins for their survival.

Key words: lead; chromium; bacteria; metallothionein; thiol

1. Introduction

Excessive heavy-metal accumulation and circulation in the biosphere are important environmental and health concerns, due to the toxicity both in essential (Cu, Cr, Zn, Mn, Fe, Ni and Mo) and xenobiotic metals (Cd, Pb and Hg) at increased levels of bioavailability [1]. Heavy metals have an important role in different biochemical reactions and are poisonous for cells in high concentrations [2]. Unlike organic contaminants which can be converted into non-toxic derivatives, metals are intrinsically persistent in nature [3]. As chromium compounds were used in dyes and paints and the tanning of leather, these compounds are often found in soil and groundwater at abandoned industrial sites. Toxic Cr (VI) is reduced to less toxic Cr (III) by bacterial system found in the industrial belt. Bioreduction of Cr (VI) has been demonstrated in several bacterial species including *Pseudomonas* sp., *Escherichia coli*, *Bacillus* sp., *Desulfovibrio* sp., *Microbacterium* sp., *Shewanella* sp., *Achromobacter* sp. and *Arthrobacter* sp. Direct bacterial reduction of Cr (VI) to Cr (III) is the most promising practice with proved expediency in bioremediation.

Because heavy metals are increasingly found in microbial habitats due to natural and industrial processes, microbes have evolved several mechanisms to tolerate the presence of heavy metals [4]. Although some heavy metals are essential trace elements, most can be, at high concentrations, toxic to all branches of life, including microbes, by forming complex compounds within the cell. Metallothioneins (MTs) are a group of low molecular mass, cysteine-rich proteins with a variety of functions including involvement in metal homeostasis, free radical scavenging, protection against heavy metal damage, and metabolic regulation *via* Zn donation [5, 6]. Owing to their rich thiol content, metallothioneins bind a number of trace elements including lead, zinc, cadmium, mercury, platinum & silver & also protects cells & tissues against heavy metal toxicity. Besides, levels of MTs in invertebrates and aquatic vertebrates well correlate with heavy metal pollution of an environment and, thus, serve as bio-environmental marker. The main objective of this study was to isolate and

---

[1] Email: *for_rini_roy@yahoo.co.in*

[2] Email: *odditybiom@gmail.com*

extract MT from the isolated bacterial culture. Induction of MT was observed in isolated bacteria upon treatment with heavy metals like lead (Pb) and chromium (Cr) at different concentrations. The thiol content was also estimated from the cell extract of the treated and untreated isolated bacteria. Probable cell metal interaction was predicted through FTIR study. Finally, MT was confirmed by SDS PAGE and Western Blotting.

2. Methodology

Among the toxic heavy metals lead (lead nitrate) and chromium (Potassium dichromate and potassium chromate) were used for studying the induction of metallothionein protein on the isolated bacteria. The concentrations used for each of the metals were 1g/L and 1.75 g/L.

2.1 Isolation of the bacteria

Bacterial cultures were isolated from a pristine soil sampled from Raniganj coal mining area, West Bengal, India using the standard dilution plate technique. A 10-fold dilutions of fresh soil (1 g) were made in phosphate buffered saline (pH7.5) and 0.1 ml from each of these dilutions were spread on minimal media agar plates supplemented with active charcoal as the sole carbon source. Plates were incubated at 37°C for 2-3 days. Colonies with different morphological appearance were selected from these culture plates and purified by further sub culturing in the same minimal media. The isolates were further grown in minimal media broths which were supplemented with Pb (II) and Chromium (VI) having concentrations 1g/L and 1.75 g/L each. 4 ml of the isolated bacterial culture was inoculated in 100 ml of Nutrient Broth since this media proved to be the growth promoting media for the successful extraction of metallothionein.

2.2 Characterization of bacteria

The organisms were characterized on the basis of detailed colony morphology, cellular arrangements, Gram nature by Bright Field Microscope, and cell motility by Phase Contrast Microscopy.

2.3 Extraction of metallothionein from bacteria

Equivalent mixtures of dithiolthreitol (DTT), phenyl methane sulfonyl fluoride (PMSF), and glycine buffer, pH=8.5 were added to 0.5 g of wet weight of above samples (harvested at the end of log phases and centrifuged at 10000 rpm for 10 min at 4 °C).Then the bacterial samples (metal treated and metal untreated) were lysed in sonicator for 3 min and cooled on ice. Then the sonicated samples were centrifuged at 10000 rpm for 10 minutes [7]. The supernatant was then further used for SDS PAGE. A minute amount of sample was kept aside for estimation of protein amount by Bradford method [8].

SDS PAGE: 12% SDS PAGE was performed using the standard protocol followed by Coomassie brilliant blue staining.

2.4 Estimation of total thiol content

For total thiol, total cell extract prepared (by taking the supernatant after centrifuging the bacterial culture at 10,000 rpm for 10 minutes) was used to measure total thiol content [9] of protein using Dithionitrobenzoic acid (DTNB), Sodium bicarbonate, Phosphate buffer – 0.1M (pH 7.4). Protein was measured by Bradford method.

FTIR study: After growth of isolated bacteria in NB, the bacterial culture was centrifuged at 10,000 rpm for 5 mins. The pellet obtained was washed with buffer and distilled water for thrice. Lyophilisation of the bacterial culture treated with or without metals was then performed. A thin uniform film of the lyophilised bacterial culture was drawn on a cover slip and FTIR was performed [10]. The IR spectra of dried whole cell were recorded with instrument having model number L1600300 spectrum Two FTIR Sl. No. 94372 (Perkin Elmer, U.S.). The sample was scanned between 600-4000 wave number in cm^{-1} at transmittance mode taking air as reference.

Western blot: Western blot technique was carried out following standard method using primary Anti Metallothionein UC1MT (ab 12228), protein marker, BCIP (5-bromo-4-chloro-3-indolyl phosphate), NBT (nitro blue tetrazolium), NBT-BCIP buffer, Secondary AP tagged antibody.

3. Discussion

Isolation of the bacteria: From the isolated bacteria grown in Nutrient Broth, further study was carried out.

Characterization of bacteria: Gram staining was done and found that the isolated culture was of gram-negative character, coccus in shape, non-motile in nature as confirmed by Phase Contrast Microscopy.

Extraction of metallothionein from bacteria: Protein was estimated from the supernatant after sonication in the extraction procedure and were then used for SDS PAGE.

SDS PAGE: 12% SDSPAGE was run using 14.3-97.4 kD protein markers. The gels were stained overnight in Coomassie Brilliant Blue R-250, fixed in 0.5% acetic acid and destained in destaining solution prior to scanning for documentation. Prominent bands could be seen in the gel, with respect to protein marker at 14 kD in control as well as in the different concentrations of Pb and Cr.

Estimation of total thiol content: From the data obtained by calculating the thiol content /mg of protein present in the cell, it could be seen that the thiol content is increasing in metal treated cultures in comparison with the control sample for both Pb and Cr. Comparing the two different metal treated cultures, it was observed that chromium treated bacteria showed higher thiol content than that of lead treated bacteria.

FTIR study: Existence of carbonyl group is high in the membrane of the organism which is supposed to interact with the metal. The shifting of peak in case of Pb and Cr shows binding of metal with the functional group on the membrane of bacteria.

Western blot: Since the protein reacted with anti-metallothionein antibody, so bands were observed, hence it was concluded that the sample contained metallothionein confirming MT induction with metal ion treatment of isolated bacteria.

4. Conclusion

From the band patterns observed in SDS PAGE with respect to the protein marker, it could be concluded that metallothionein activity is induced in lead treated and the chromium treated cultures. Thiol content was increased due to heavy metal challenge in all the cases for Pb and Cr. It can be concluded that isolated bacteria possess metal tolerance capacity by induction of metallothionein protein. One of the useful aspects could be the use of the isolated bacteria to clean up metal contaminated sites, viz; lead and also for Chromium (VI) contaminated site such as in industrial wastes.

Acknowledgement: The work was executed in the Post Graduate Department of Microbiology, Lady Brabourne College. The authors are grateful to Dr. Suchandra Majumdar, Bose Institute for her help in Western Blotting and to Department of Microbiology and Chemistry, Maulana Azad College for lyophilization and FTIR study, respectively.

References:

1. J.O. Nriagu and J.M. Pacyna, *Nature* **333** (1988) 134.
2. D.H. Nies, *Appl. Microbiol. Biotechnol*. **51** (1999) 730.
3. M. Valls, S. Atrian, V. de Lorenzo and L.A. Fernández, *Nat. Biotechnol*. **18** (2000) 661.
4. I.V.N. Rathnayake, M. Meghraj, N. Bolan and R.Naidu, *Int. J. Civ. Env. Engg*. **2** (2010) 191.
5. N. Shiraishi et al., *Toxicol. Appl. Pharmacol*. **85** (1986) 128.
6. N. Shiraishi, K. Aono and K. Utsumi, *Radiat. Res*. **95** (1983) 298.
7. M. Enshaei, A. Khanafari and A. AkhavanSepahy, *Iran. J. Environ. Health. Sci. Eng*. **7** (2010) 287.
8. M.M. Bradford, *Anal. Biochem*. **72** (1976) 248.
9. G.L. Ellman, K.D. Courtney, V. Andres and R.M. Featherstone, *Biochem. Pharmacol*. **7** (1961) 88.
10. Y. Chen et al., *Food Chem*. **107** (2008) 231.

Scientific Voyage
Vol. 1, No. 4,
Page 28-33 (2020)

SCIENTIFIC VOYAGE
ISSN: 2395-5546

GCECT
Publication
Oct.-Dec.

Pneumonia Detection based on X-ray image classification using Convolutional Neural Network based Deep Learning Model

Subrata Sarkar [a1], Alok Mukherjee [a2], Kingshuk Chatterjee [a3], Partha Haldar [a4]

[a] *Government College of Engineering and Ceramic Technology, Kolkata 700010, West Bengal, India*

Abstract. Pneumonia is a disease that threat humanity to this day. Even though we have developed vaccines and medicines, many lives are still lost every year due to this disease. So we have made an effort to develop an algorithm which would be able to detect this disease in an early stage to help people with the diagnosis. We have developed a Convolutional Neural Network (CNN) based Deep Learning (DL) model that detects pneumonia from the X-ray image of patients. This helps in classifying a given image, which, in turn, helps the physicians and other medical persons for easier diagnosis. In this study we have compared the outputs from two CNN based DL models: a 3 layered model and another 10 layered model. We have taken the chest x-ray images of different patients for developing and testing the proposed algorithm in Python platform.

Keywords: Pneumonia, X-ray image, Convolutional Neural Network (CNN), Deep Learning, Image classification.

1. Introduction

Pneumonia is an infection that inflames the alveoli in one or both lungs. These may be filling up with fluid or pus, causing cough with phlegm or pus; causing fever and difficulty breathing. Tuberculosis is a potentially infectious disease usually caused by Mycobacterium tuberculosis bacteria. Tuberculosis generally affects the lungs, but can also affect other parts of the body. Accurate diagnosing of pneumonia is thus extremely important. Chest radiograph (CXR) or chest X-ray is usually examined by trained specialists. Handling of the huge number of patients every day in the hospitals and clinics would greatly be assisted by a technique, which would perform a basic screening for Pneumonia detection.

Machine learning based solutions are developing every day for helping the clinicians and physicians more efficiently in correct prediction. So we have tried to develop two deep learning based models. These two designed Convolutional Neural Network (CNN) based models are found to predict pneumonia with a high accuracy of 90% approximately. This proposed method is intended to enable technicians to increase their efficiency, as well as, reduce their effort. At the same time, this would enable fast initial prediction of the disease and allow patients to consult with a physician immediately on detecting any positive result from the algorithm. We have used Keras with tensorflow backend to create the proposed convolutional neural network model. This is followed by training the proposed deep learning model using the open source image data from Kaggle. Finally, the model is validated using images from the same source. We have tried to develop a model which doesn't possess any addition computational intricacy apart from the CNN based deep learning method, which is used as the basic computational tool. Simultaneously, we have tried to retain an acceptable accuracy level, with high specificity so that it can be used as a everyday computation devices or can be handled by weaker computers very easily. These would also help diagnosis in the rural areas especially, where deficiency of computers with superior computational features or high level medical facility is a major hindrance to medical treatment.

---

[1] E-mail: *subrotosarkar32@gmail.com*
[2] E-mail: *alokmukherjee.ju@gmail.com*
[3] E-mail: *kingshukchaterjee@gmail.com*
[4] E-mail: *partha.jumech@gmail.com*

There have been initiatives to develop openly available databases of medical image with the ever increasing demand of medical support, as well as, increasing numbers of patient in the recent few years. OpenI [1] holds one of such open datasets, particularly for chest X-rays. This contains 3,955 (nearly four thousand) radiology reports from the Indiana Network for Patient Care and 7,470 (more than seven thousand) number of chest x-rays from the different hospitals in their picture archiving and communication system (PACS). Pneumonia is usually diagnosed using the increased opacity on CXR [2]. CXRs are the most usual tool used for the diagnostic imaging study by the physicians. But this imaging technique has several influencing factors; like the positioning of the patient during the X-ray imaging, or the depth of inspiration causing variation in the air volume inside lungs are responsible for altering the image quality of the CXR [3]. This further complicates the interpretation of the image, especially with naked eye. In the proposed work, we have used images from the Cell Press [4] on kaggle and images compiled by Kevin Mader [5] on kaggle. CheXnet is one of the recently developed state-of-the-art methods which has a very high level of accuracy of disease detection [6]. Recent advances in the field of deep learning incorporating features of convolutional neural network, especially using activation maximization and other techniques, have given a new direction to the studies, as well as, a new dimension of application of the neural networks.

2. Methodology

We have developed two neural network models in the proposed work. One of the models is a shallow 3 layered network and the other is a 10 layered network. We have described the structure of each of the networks and visualized their filters and class activation mappings in the following sections.

2.1 Algorithm of the proposed models

Model 1: This is a 10 layered CNN model. We have used data sets from kaggle for training our model. We have used 80:20 split for training and testing. The architecture of the model is briefly described here:

Model: "sequential_1"

Layer (type)	Output Shape	Param #
conv2d_1 (Conv2D)	(None, 98, 98, 32)	896
batch_normalization_1 (Batch	(None, 98, 98, 32)	128
conv2d_2 (Conv2D)	(None, 96, 96, 32)	9248
batch_normalization_2 (Batch	(None, 96, 96, 32)	128
conv2d_3 (Conv2D)	(None, 48, 48, 32)	25632
batch_normalization_3 (Batch	(None, 48, 48, 32)	128
dropout_1 (Dropout)	(None, 48, 48, 32)	0
conv2d_4 (Conv2D)	(None, 46, 46, 64)	18496
batch_normalization_4 (Batch	(None, 46, 46, 64)	256
conv2d_5 (Conv2D)	(None, 44, 44, 64)	36928
batch_normalization_5 (Batch	(None, 44, 44, 64)	256
conv2d_6 (Conv2D)	(None, 22, 22, 64)	102464
batch_normalization_6 (Batch	(None, 22, 22, 64)	256
dropout_2 (Dropout)	(None, 22, 22, 64)	0
conv2d_7 (Conv2D)	(None, 20, 20, 128)	73856
batch_normalization_7 (Batch	(None, 20, 20, 128)	512
conv2d_8 (Conv2D)	(None, 18, 18, 128)	147584
batch_normalization_8 (Batch	(None, 18, 18, 128)	512
conv2d_9 (Conv2D)	(None, 9, 9, 128)	409728
batch_normalization_9 (Batch	(None, 9, 9, 128)	512
dropout_3 (Dropout)	(None, 9, 9, 128)	0
conv2d_10 (Conv2D)	(None, 6, 6, 256)	524544
batch_normalization_10 (Batch	(None, 6, 6, 256)	1024
flatten_1 (Flatten)	(None, 9216)	0

```
dropout_4 (Dropout)          (None, 9216)          0
dense_1 (Dense)              (None, 2)             18434
=================================================================
Total params: 1,371,522
Trainable params: 1,369,666
Non-trainable params: 1,856
```

Model 2: This is a 3 layered CNN model. We used data-sets from kaggle for training our model. We have used 80:20 split for training and testing. Here is the architecture of the model:

```
Model: "sequential_1"
_________________________________________________________________
Layer (type)                 Output Shape              Param #
=================================================================
conv2d_1 (Conv2D)            (None, 98, 98, 32)        896
batch_normalization_1 (Batch (None, 98, 98, 32)        128
conv2d_2 (Conv2D)            (None, 49, 49, 32)        25632
batch_normalization_2 (Batch (None, 49, 49, 32)        128
dropout_1 (Dropout)          (None, 49, 49, 32)        0
conv2d_3 (Conv2D)            (None, 25, 25, 64)        51264
batch_normalization_3 (Batch (None, 25, 25, 64)        256
dropout_2 (Dropout)          (None, 25, 25, 64)        0
flatten_1 (Flatten)          (None, 40000)             0
predictions (Dense)          (None, 2)                 80002
=================================================================
Total params: 158,306
Trainable params: 158,050
Non-trainable params: 256
```

The proposed models are next tested to identify its accuracy, specificity, f1-score and Mathew's Correlation Coefficient (MCC). Testing is carried out for both the 3 layered and 10 layered CNN models. A comparison is carried out between the two models by judging the outputs. We have used Keras with tensorflow backend in python domain as the major computational tool to carry out the algorithm design.

3. Results and Discussion

3.1 Results for pneumonia detection

The outcomes of the proposed models are described in Table 1. A comparative analysis of the two proposed models could also be obtained from this table. It shows that the 10 layered CNN architecture produces much higher accuracy and sensitivity compared to the 3 layered model.

Table 1. Comparative analysis of the two proposed CNN models

Models	*Accuracy*	*Sensitivity*	*Specificity*	*F1-score*	*MCC*
Custom model 10 layers	0.9539	0.9713	0.9037	0.9691	0.8788
Custom model 3 layers	0.9283	0.9311	0.9203	0.9508	0.8218

The metrics for training the models are explained next. Apart from that, the metrics on how the models performed on test data is also discussed. Training of the 10 layered model has been carried out for 60 epochs and the 3 layered model has been trained for 30 epochs.

3.2 Custom model of 10 layers

The outcomes of the custom model of the 10 layer CNN architecture is shown graphically in Fig. 1, which illustrate the variation in loss and accuracy of the model for the 60 epochs, obtained for both validation and testing the model. The results are also represented in table 2. It is also observed that the accuracy of the model increases almost monotonically with increase in the number of epochs.

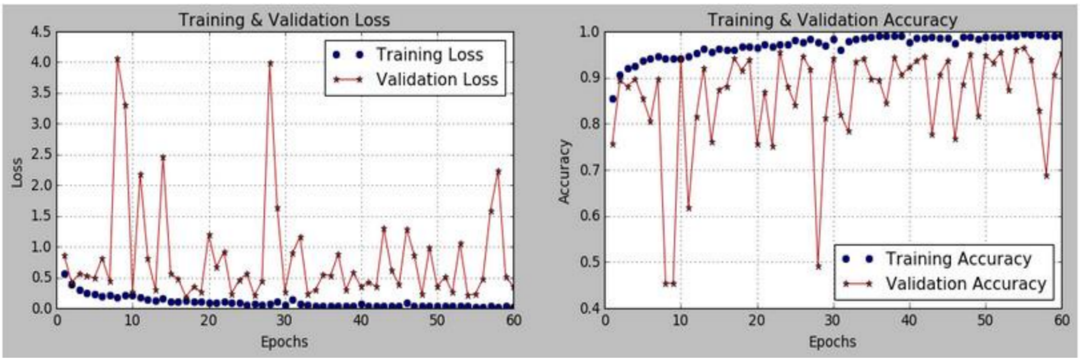

(a) (b)

Fig. 1: Outcomes of the 10 layer CNN architecture showing (a) Loss and (b) Accuracy

Table 2. Outcomes of the 10 layers CNN model

Test Accuracy = 0.954				
	precision	***recall***	***f1-score***	***support***
class 0 (abnormal)	0.97	0.97	0.97	871
class 1 (normal)	0.92	0.9	0.91	301
Accuracy			0.95	1172
Macro average	0.94	0.94	0.94	1172
Weighted average	0.95	0.95	0.95	1172

The confusion matrix, without normalization, is also found as: $\begin{bmatrix} 846 & 25 \\ 29 & 272 \end{bmatrix}$. This is also shown in Fig. 2

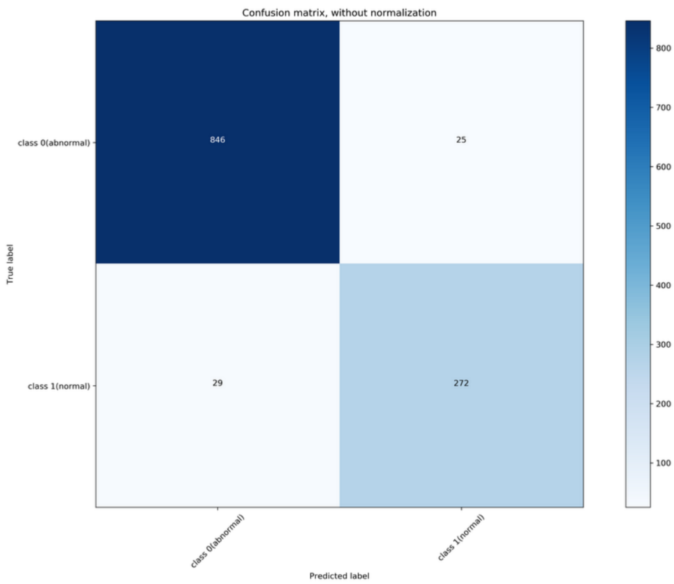

Fig. 2: Confusion matrix of the custom model of 10 layers

3.3 Custom model of 3 layers

The outcomes of the custom model of the proposed 3 layer CNN architecture is shown graphically in Fig. 3. These figures again illustrate the variation in loss and accuracy of the model, but this time for 30 epochs only.

These are again obtained for both validation and testing the model. The results are again represented in tabular form in table 3. Again it is observed that the accuracy of the model increases almost monotonically, like that of the proposed 10 layer model, with increase in the number of epochs.

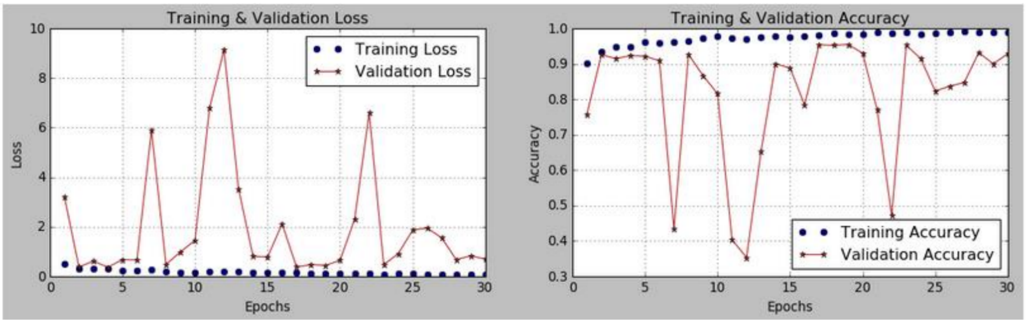

(a) (b)

Fig. 3. Outcomes of the 3 layer CNN architecture showing (a) Loss and (b) Accuracy

Table 2. Outcomes of the 10 layers CNN model

Test Accuracy = 0.923				
	precision	***recall***	***f1-score***	***support***
class 0 (abnormal)	0.97	0.93	0.95	871
class 1 (normal)	0.82	0.92	0.87	301
Accuracy			0.93	1172
Macro average	0.90	0.93	0.91	1172
Weighted average	0.93	0.93	0.93	1172

It is clearly observed by comparing Table 1 and Table 2 that the proposed 10 layer model outperforms the 3 layer model in most of the fields. This easily explains the superiority of the proposed 10 layer model over the 3 layer model. The confusion matrix, without normalization, is also found as: $\begin{bmatrix} 811 & 60 \\ 24 & 277 \end{bmatrix}$.
This is again shown in Fig. 4.

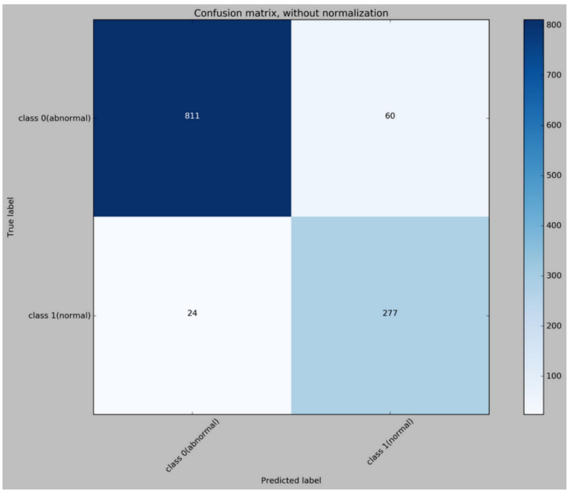

Fig. 4. Confusion matrix of the custom model of 3 layers

4. Conclusion

Two Convolutional Neural Network (CNN) models are proposed in this work to develop an algorithm for the detection of Pneumonia, using the Chest radiograph (CXR) or chest X-ray images. Results show that both the proposed CNN models perform satisfactorily; although, the superiority of the 10 layer CNN architecture is well established. The metrics for the test dataset again prove that both the CNN models are effective for image classification. Both of the custom models have been tested using Flask locally. The present work shows a good prosperity for easy implementation in medical field, especially where low computational analysis is the most important factor. Easy, fast and efficient detection of pneumonia disease using the proposed models would help in an efficient initial screening; thereby faster diagnosis of patients. Thus the model shows good prosperity for implementation in real world.

References:

1. X. Wang, Y. Peng, L. Lu, Z. Lu, M. Bagheri, R.M. Summers, ChestX-ray8: Hospital-scale Chest X-ray Database and Benchmarks onWeakly-Supervised Classification and Localization of Common Thorax Diseases; http://openaccess.thecvf.com/content_cvpr_2017/papers/Wang_ChestX-ray8_Hospital-Scale_Chest_CVPR_2017_paper.pdf.

2. T. Franquet, Imaging of community-acquired pneumonia (J. Thorac Imaging 2018, epub ahead of print, PMID 30036297.

3. B. Kelly, The Chest Radiograph, *Ulster Med. J.* **81** (2012) 143.

4. D.S. Kermany et al., Identifying Medical Diagnoses and Treatable Diseases by Image-Based Deep Learning; https://www.cell.com/cell/fulltext/S0092-8674(18)30154-5.

5. K. Mader, Pulmonary Chest X-Ray Abnormalities; https://www.kaggle.com/kmader/pulmonary-chest-xray-abnormalities.

6. P. Rajpurkar et al., CheXNet: Radiologist-Level Pneumonia Detection on Chest X-Rays with Deep Learning; https://arxiv.org/abs/1711.05225.

Scientific Voyage
Vol. 1, No. 4,
Page 34-40 (2020)

SCIENTIFIC VOYAGE
ISSN: 2395-5546

GCECT
Publication
Oct.-Dec.

Bibhutibhusan Dutta: A Sage Mathematician

Utpal Mukhopadhyay[1]
Satyabharati Vidyapith, Nabapally, North 24 Parganas, Kolkata 700 126, West Bengal, India

Abstract: Bibutibhusan Dutta (Swami *Vidyaranya* in later life), a successful professor of mathematics, has glorified India by bringing in limelight the significant contributions of Indian mathematicians of ancient period as well as doing high level mathematical research in applied mathematics. In this work, life and scientific contributions of Prof. Dutta have been discussed with special emphasis on history of mathematics of ancient India.

Keywords: Mathematics; ancient Indian mathematics; applied mathematics

1. Introduction

The year 1888 is a significant milestone for India because two luminaries of our motherland, viz. Dr. Sarvapalli Radhakrishnan (1888-1975), a world famous philosopher as well as the second President of India and the Nobel Laureate physicist Sir C.V. Raman (1888-1970) were born in that eventful year. But most of us either do not know or have forgotten that Bibhutibhusan Dutta (1888-1958), another great son of India who glorified our country by highlighting the significant contributions of ancient Indian mathematicians, saw the light of this world in the same year. Through his in-depth research work, he presented before the world the origin and subsequent developments of various mathematical ideas made by our ancestors starting from the Vedic period.

Fig. 1: Bibhutibhusan Dutta

----
[1] Email: *utpalsbv@gmail.com*

Fig. 2: Father Rasik Chandra Dutta and Mother Muktakeshi Devi

2. Biographical Sketch

Biographical facts are drawn largely from [1] unless mentioned otherwise. Bibhutibhusan Dutta, the third son of Rasik Chandra Dutta (1854-1926) and Muktakeshi Devi (1861-1958), was born on 18 June, 1888 at Kanungopara of Chittagong in undivided India (now in Bangladesh). It may be mentioned that in the previous year legendary mathematician Srinivas Ramanujan (1887-1920) was born. Rasik Chandra was a Government servant in Chittagong court. He had eleven sons and four daughters. Although Rasik Chandra had to pass a life of extreme hardship and financial stringency, he was fortunate enough that each of his eleven sons was a jewel. The eldest son Rebatiraman (M.A.) was a Deputy Magistrate, second son Bhupatimohan (M.A.B.L.) a lawyer, Bibhutibhusan (D.Sc., P.R.S.) a professor, Nirodlal (M.B.) a physician, Benodbehari (Ph.D., P.R.S.) Controller of Examination of Calcutta University, Harihar (M.B.) a physician, Pramatha (Ph.D.) a professor, Subimal (I.A.S.) Indian Ambassador, Sukomal (B.Sc., Engg.) an engineer, Parimal (M.B.) a radiologist and youngest son Ranajit (B.E.) was an engineer. For giving birth to so many great sons, Muktakeshi became known as a 'golden womb lady' (*ratnagarva* in Bengali).

Bibhutibhusan loved his father so much that he stayed with him at Rasik Chandra's working place in a remote area 30 km away from Chittagong town devoid of any institution. So, beginning of formal education of Bibhutibhusan was delayed by nearly three years. After Rasik Chandra was transferred to Chittagong town, Bibhutibhusan entered the Chittagong Municipal School and passed Matriculation Examination in 1907 with District Scholarship. Then he entered Presidency College (now a University), Kolkata in I.Sc. course. In 1909 he passed I.Sc. Final Examination in first division but failed to win scholarship. Then he took admission in the same college in B.Sc. course with Honours in mathematics. In the B.Sc. final examination in 1911, he performed well in theoretical papers, but his result in the practical examination was not up to his expectation. So, he had to appear again in the same examination in 1912 and obtained second class honours. It should be mentioned here that his performance in the I.Sc. and B.Sc. examinations were not proper indicators of his talent. His two papers were accepted for publication even before his graduation was completed. In fact, his too much inclination towards the religious world proved costly so far as his academic career is concerned. However, in 1914 Bibhutibhusan secured first class in M.Sc. Examination in Mixed Mathematics (presently Applied Mathematics) from Calcutta University. It is interesting to note that seven months before his M.Sc. final examination, Bibhutibhusan suddenly disappeared from his mess in Kolkata. After a tiring effort of his eldest brother Rebatiraman, he was traced at Haridwar where he went for asceticism. Rebatiraman brought him back to Kolkata and in spite of this distraction from his studies, Bibhutibhusan was talented enough to obtain first class in M.Sc. final examination.

Even before publication of result of M.Sc. Examination, Bibhutibhusan published a short research paper which drew attention of Sir Asutosh Mukherjee (1864-1924), the then Vice-Chancellor of Calcutta University. Being a great mathematician himself, Asutosh readily recognized excellence of Bibhutibhusan and in 1915 granted him a research scholarship of Rs. 75/- per month. In 1916 he was appointed as an assistant to famous mathematician Ganeshprasad (1876-1935), the then Rashbehari Ghosh Professor of mathematics in Calcutta University. At that time Bibhutibhusan had to take some classes of M.sc. course. He became Premcahand Roychand Scholar (PRS) in the year 1917. The entire amount of the scholarship was awarded to him because the standard of his article was much higher than other candidates. Being a PRS he received Mouat Medal. He was awarded Elliot Prize also. He obtained D.Sc. degree from Calcutta University by working on problems related to hydrodynamics.

In the session 1917-18, Bibhutibhusan got an appointment as lecturer of Mixed Mathematics in the University of Calcutta. In that golden era of Calcutta University, a group of highly talented youth, viz. S. N. Bose (1894-1974), M.N. Saha (1893-1956), N.R. Sen (1894-1963), N. Basu, S. Banerjee etc. were colleagues of Bibhutibhusan. When Ganeshprasad resigned from his Professorship in 1919, Dr. S. Banerjee succeeded him till 8 April, 1922. When Prof. Banerjee also resigned the Chair was offered to Prof. Dutta. According to Dutta's brother Benodebehari, after resignation of Dr. Banerjee, Bibhutibhusan was offered the post but he declined by saying: "*After a couple of days I shall become sannyasi [and so] I have no need for the promotion*" [2]. But, as no other befitting person was found for that post, Prof. Dutta agreed to accept the offer for a brief period but declined to receive any extra remuneration. This incident proves the generosity of Bibhutibhusan and this type of sacrifice is rare now-a days. As a teacher, Prof. Dutta was very successful and he could teach efficiently any topic included in the syllabus. He also successfully performed his duty as a Secretary of the Calcutta Mathematical Society (CMS), the brainchild of Sir Asutosh Mukherjee. In the 20th Foundation Year Celebration of the CMS in 1928 Ganeshprasad paid his respect to Bibhutibhusan by saying: *"But I consider it my duty to state that but for the devotion of Dr. Bibhutibhusan Dutta, who at the earnest request of Sir Asutosh Mukherjee in 1924 undertook to shoulder the responsibility of a Secretary, the Society would have found it extremely difficult to publish so many volumes of journals as it did in last four years"*. Incidentally at that time Asutosh was not in this world to witness that he rightly handed over the responsibility of his dear CMS to a befitting person. In the last years of 1920s B. B. Dutta became irregular in his teaching profession and went on leave during 1928-1930. Ultimately he resigned from his post in 1931 to become a *sannyas*i. In April, 1932 he wrote a review article on '*Siddhantasekhar*'. Finally, since 1933 he detached himself from all kind of activities related to the university and received the Order of *Sannyas* on 17 February, 1938 in Chittagong by accepting Swami Vishnu Tirthji Maharaj (1889-1969) as his Guru [3] and since then he became known as *Swami Vidyaranya*. After staying hither and thither for some time, he ultimately settled at Puskar near Ajmer of Rajasthan where he spent the rest of his life at that place until his demise on 6 October, 1958. It may be mentioned here that his brother Nirodlal, who was a renowned physician, also became a *sannyasi* and his ancestor Mukundaram was a close associate of Sri Chaitanyadeb (1486-1534). B.B. Dutta wrote two books on Indian religion and philosophy which were published posthumously [4, 5].

3. Scientific Contributions

It has already been mentioned that Bibhutibhusan obtained his D.Sc. from Calcutta University by working on hydro-dynamical problems. His thesis contained eight papers which were published in Philosophical Magazine (London), American Journal of Mathematics, The Tohokuo Mathematical Journal etc. Apart from the thesis papers, he wrote some more papers on mainstream mathematics. After resigning from his service, he left the path of hardcore mathematical research and entered into the field of history of mathematics. So, B. B. Dutta's research works can be classified into two major fields, viz. (1) mainstream research in Applied Mathematics and (2) history of mathematics in ancient India. The period of his hardcore research spanned from 1910-11 to 1921, i.e. about ten years. After this period he focused his attention towards ancient Indian mathematics.

3.1 Research in Applied Mathematics

Prof. Dutta worked mainly on fluid dynamics and theory of elasticity. The main characteristics of his research were extraction of physical significance of fundamental theories. For instance, in his maiden publication he showed that proper interpretation of some formulae in elasticity theory in a homogeneous medium might explain the theory of gravitation [6]. In the next paper, considering a law of gravitation of the form $F = -\mu/r^k$ he showed that an ellipsoidal figure can be a surface of equilibrium only when $k = -1$ [7]. Then he also investigated by assuming the law of gravitation as $F = -k^3/r^2 - \mu r$. Some of the results obtained by Prof. Dutta were related as well as applicable to real life. For instance, he proposed a method of determining the non-stationary state of heat in an ellipsoid [8] and in that process with the help of solid harmonics he generalized the equation of elliptic surfaces. In that work, he also calculated the changes in the thermal field perpendicular to the elliptic plane. In the context of this work it may be mentioned here that the solution of physical problems related to elliptical and spherical surfaces can be applied for antenna and other electrical devices. B.B. Dutta made significant contributions in the field of fluid mechanics. He studied the motion of two spheroids in an infinite liquid [9, 10]. Using judicious mathematical techniques he investigated the stability of circular and rectilinear vortices [11, 12]. In two successive papers, Prof. Dutta studied the behavior and periods of vibrations of vortices [13, 14]. He had two publications on spherical harmonics also [15,16].

3.2 Reasearch in Ancient Indian Mathematics

In spite of his important contributions in Applied Mathematics, Prof. B.B. Dutta is remembered chiefly for his seminal work on history and development of ancient Hindu and Jain mathematics. He had nearly sixty research publications in this direction which were published in foreign journals, viz. American Mathematical Monthly, Bulletin of American Mathematical Society, Quellen und Studien zur Gaschichte der Mathematik, Archeion and

Scientia as well as in various Indian journals. In colonial India, contributions of Indian mathematicians were mostly underestimated by Western scholars of history of mathematics. To them, Indian mathematics was nothing more than astrology and Indian mathematicians are indebted to Greek mathematics. Under this situation, Prof. Dutta, being inspired by Prof. Ganesh Prasad (a pioneer in India for research work in history of mathematics), took up the task of highlighting achievements of ancient Indian mathematicians. In this work he was supported by Avdhesh Narayan Singh, a student of Prof. Ganesh Prasad. Dr. Singh, after obtaining M.Sc. degree from Benaras Hindu University in 1924, came to Calcutta around 1926 and received D.Sc. degree in 1928 from Calcutta University working under the supervision of Prof. Ganesh Prasad. During his stay at Calcutta, Dr. Singh used to visit Dr. Dutta in his mess for getting some direction and help from him. In this way Dr. Singh had some intimacy with Dr. Dutta. After resigning from his service, Prof. Dutta left the path of hardcore mathematical research and entered into the field of history of mathematics. He went on to explore the contributions of ancient Indian mathematicians. In fact he started publishing papers in this field since 1920. But he entirely engaged himself in this area of research near the end of 1920s. B. B. Dutta observed that many researchers had a tendency to show the indebtedness of India to Greek and Arab mathematicians. Those scholars arrived at their conclusion without going into details and misinterpreting the available resources. Moreover there were a number of commentaries of great masters like Aryabhatta, Brahmagupta, Bhaskaracharya II etc which differed slightly from each other. So, Prof. Dutta had an uphill task of going through the primary resources which were written in Sanskrit. Since he had proficiency in Sanskrit, he could extract the real meaning of the literature, written mainly in the form of '*slokas*'.

In the year 1926, Prof. Dutta's first five papers on the history of mathematics were published [17-21]. His lecture entitled *Contributions of the Ancient Hindus to Mathematics* at Allahabad University on December 27, 1927 was subsequently published in the Bulletin of the Allahabad Mathematical Association [22]. Prof. Dutta firmly established that ancient Hindu mathematicians had a deep knowledge in geometry; otherwise it was impossible for them to construct altars of various shapes meant for religious observances. Not only that, he showed clearly that Hindu geometry was earlier than Greek geometry of Hellenistic era, regarded as the golden period of geometry in Greece. In his article *Hindu Origin of Geometry*, Prof. Dutta wrote: "*The Hindu geometry commenced at a very early period, certainly not later than that in Egypt, probably earlier, in construction of altars for the Vedic sacrifice……In course of time, it however, grew beyond its original sacrificial purpose or the limits of practical utility and began to be cultivated as a science for its own sake. Indeed, there is no doubt about the fact that the study of geometry as a science began first in India. Further, the early Hindu geometry was much in advance of the contemporary Egyptian or Chinese geometry. The Greek geometry was yet to be born*" [2]. According to Dutta, ancient Hindus used ropes (*sulba* in Sanskrit) for constructing altars of specific configurations. So they had written the method of constructing various altars (using ropes) in the form of *slokas* which were called '*sulba sutra*' At that time Boudhayana, Katyana, Apastamba, Manab etc. were famous '*sulbakars*', i.e. geometers in modern sense [23].

Prof. Dutta established that for constructing altars the ancient Hindu mathematicians had to master the process of dividing any figure into a number of parts, the method of drawing a perpendicular on a straight line, the process of finding three suitable numbers satisfying Pythagoras theorem $x^2 + y^2 = z^2$ etc. Moreover, they could find the approximate values of $\sqrt{2}$ and π. In fact, Boudhayana and Apastamba derived the value of square root of 2 correct to five decimal places which were unknown to Greek mathematicians of contemporary period.

Similarly, Prof. Dutta proved that Arabs learnt algebra from the Hindus. In his paper *Origin of Algebra* [2] he wrote: "*The science of algebra derived its name from the title of a certain work by the Arab Mahammad bin Musa Alkhowarizmi, viz. al-gebr-w'al-mugabalah, which contains an early systematic treatment of the general subject as distinct from the science of numbers……But the subject matter of Alkhowarizmi's treatise was not his original contribution. He got it from the Hindus*". Regarding the use of calculus, Dutta reasoned that the word *Tatkalika gati* (instantaneous motion) found in the works of Manjula, Aryabhatta II and Bhaskara II are nothing but the idea of differentials.

Prof. Dutta encapsulated all these works in his magnum opus *The History of Hindu Mathematics* in three volumes. After his premature retirement from Calcutta University, Prof. Dutta handed over the manuscripts of those volumes to his younger assistant Avadhesh Narayan Singh who published first two volumes in 1935 and 1938 respectively [24, 25] from Lahore. Afterwards, in 1962 this book (Part I and II) was published again by Asia Publishing House. In the third part of this book, contribution of Hindus in geometry, in the development of trigonometry, calculus, permutations and combinations, surds, series and magic squares were discussed. Dr. Singh could not publish the third volume due to his premature death in 1954 and it was never published as a book. However, due to sincere effort and editing by Dr. Kripasaran Shukla, Professor of mathematics of Lucknow University, it was published serially in Indian Journal of History of Science as separate papers during 1980-1993 [26-32]. In his review of History of Hindu Mathematics (Part I) L. G. Simons, a renowned historian of mathematics, has commented: "*Datta and Singh's History of Hindu Mathematics should be in every library which reaches standards covered by the word 'approved'. It should be owned by individuals who have any interest whatever in the history of the progress of science. From the standpoint of authoritative subject matter and from that of book-making, it is a notable history*" [2, 33]. Part I of the book deals with history and development of Hindu numerals in the place value system as well as other numerals followed by Hindu mathematicians. Prof. Dutta strongly opined that the term 'Hindu-Arabic numerals' should be replaced by 'Hindu numerals'. Second part of the book deals with the process of obtaining general solutions in rational integers of indeterminate and bi-quadratic equations. But prior to writing this book, in the year 1931, being invited by Ganesh Prasad, Prof. Dutta delivered six lectures on ancient Hindu geometry. Those lectures were compiled in the book *The Science of Sulva: a Study of Hindu Geometry*. Dr. Dutta wrote (28 July, 1932) in the preface of this book: "*I tender grateful thanks to Mr. A. C. Ghatak, Superintendant and to the staff of the Calcutta University Press for kindly expediting the publication of the book in order to help me to go back to my retirement earlier*". It was published by the University of Calcutta. Raymond C. Archibold (1875-1955), a scholar in History of Mathematics, has commented on this book: "*Dr. Dutta's volume should be in the hands of every student of the history of mathematics*" [33, 34]. Finally it should me mentioned that B. B. Dutta had publications on ancient Jain mathematics also [34, 35].

4. Conclusion

Great minds spend their lives for fulfilling some missions. Prof. B. B. Dutta also had two missions- mathematical research (including history of mathematics) and religious activity. No doubt, he could fulfill both his dreams. In the first part of his life, in spite of a spiritual inclination, he concentrated mainly on his academic career and mathematical research. Then he delved into history of ancient Hindu mathematics which, most probably, was motivated by his patriotism. Finally he detached himself from mundane attractions and led his life as a sage. So, the life of Prof. Dutta can be regarded as that of a mathematician in the cocoon of a sage. His contributions in reviving the glorious past of India in mathematical science should be remembered for ever.

References:

1. *Ganitagya Bibhutibhusan tatha Swami Vidyaranya*; edited by Sukomal Dutta (Calcutta, 1990).
2. R.C. Gupta, *Historia Mathematica* **7** (1987) 126.
3. R.C. Gupta, *Math. Student* **55** (1987) 117.
4. B.B. Dutta, *Ancient History of Bhagabata Religion* (4 volumes in Bengali, 1963-66).
5. B.B. Dutta, *Ancient Story of Advaita Philosophy* (in Bengali, 1972).
6. B.B. Dutta, *Bull. Cal. Math. Soc.* **2** (1910-11) 19.
7. B.B. Dutta, *Bull. Cal. Math. Soc*. **3** (1911-12) 21.
8. B.B. Dutta, *Am. J. Math*. **41** (1919) 133.
9. B.B. Dutta, *Bull. Cal. Math. Soc*. **7** (1915) 49.
10. B.B. Dutta, *Am. J. Math.* **43** (1921) 134.
11. B.B. Dutta, *Phil. Mag.* ***40*** (1920) 138.
12. B.B. Dutta, *Bull. Cal. Math. Soc*. **10** (1920) 219.
13. B.B. Dutta, *Proc. Benares Math. Soc*. **2** (1920) 23.
14. B.B. Dutta, *Proc. Benares Math. Soc*. **3** (1921) 13.
15. B.B. Dutta, *Tohoku Math. J.* **15** (1919) 166.
16. B.B. Dutta, *Tohoku Math. J.* **17** (1920) 210.
17. B.B. Dutta, *Proc. Benaras Math. Soc*. **7** (1926) 9.

18. B.B. Dutta, *Am. Math. Mon*. **33** (1926) 220.
19. B.B. Dutta, *Bull. Cal. Math. Soc*. **17** (1926) 59.
20. B.B. Dutta, J. *Asiatic Soc. Beng*. **22** (1926) 25.
21. B.B. Dutta, *Am. Math. Mon*. **33** (1926) 449.
22. B.B. Dutta, *Bull. Allahabad Math. Assoc*. **1** (1927) 49.
23. B.B. Dutta, *Quellen und studies Zur Geschichte der Mathematik* B **1** (1929) 245.
24. B.B. Dutta and A.N. Singh, *History of Hindu mathematics: A Source Book*, Part I (M.B. Das, Lahore, 1935).
25. B.B. Dutta and A.N. Singh, *History of Hindu mathematics: A Source Book*, Part II (M.B. Das, Lahore, 1938). Motilal Banarasi Das, Lahore.
26. B.B. Dutta, *Ind. J. Hist. Sci*. **15** (1980) 121.
27. B.B. Dutta, *Ind. J. Hist. Sci*. **19** (1984) 95.
28. B.B. Dutta, *Ind. J. Hist. Sci*. **27** (1992) 51.
29. B.B. Dutta, *Ind. J. Hist. Sci*. **27** (1992) 231.
30. B.B. Dutta, *Ind. J. Hist. Sci*. **28** (1993) 103.
31. B.B. Dutta, *Ind. J. Hist. Sci*. **28** (1993) 253.
32. B.B. Dutta, *Ind. J. Hist. Sci*. **28** (1993) 265.
33. J. J. O'Connor and E. F. Robertson, *Mac Tutor History of Mathematics*, mathhistory.st-andrews.ac.uk
34. R.C. Archibald, *Isis* **22** (1934) 272.
35. B.B. Dutta, *Bull. Cal. Math. Soc*. **21** (1929) 115.

Scientific Voyage
Vol. 1, No. 4,
Page 41-42 (2020)

SCIENTIFIC VOYAGE
ISSN: 2395-5546

GCECT
Publication
Oct.-Dec.

ERRATUM

An overview of cybersecurity risks during the COVID-19 pandemic period

Soumit Chowdhury [1], Soumya Mukherjee [2], Saranya Naha Roy [3], Rashed Mehdi [4] and Rishav Banerjee [5]

Department of Computer Science and Engineering, Government College of Engineering and Ceramic Technology, Kolkata 700010, West Bengal, India

---

The original publication of the article contained missing attribution to one table on page 49. The corresponding attribution for the same has been corrected in this version.

Two graphs represented on page 50 and 51 have been redone in order to remove branding from the surveying company. However, the attribution for the same has also been mentioned.

1(a):

Table 1: Cyber-dependent crime and online fraud record in May 2019 and May 2020 on page 49 will be replaced by:

Table 1: Cyber-dependent crime and online fraud record in May 2019 and May 2020 [1] (Source: Buil-Gil et al. (2020)).

1(b):

Table 2: Cyber-dependent crime and online fraud record in May 2019 and May 2020 on page 49 will be replaced by:

Table 2: Cyber-dependent crime and online fraud record in May 2019 and May 2020[1] (Source: Buil-Gil et al. (2020)).

----
[1] E-mail: *joy_pinu@yahoo.co.in*
[2] E-mail: *soumyamukherjee@mail.com*
[3] E-mail: *saranyanaharoy@gmail.com*
[4] E-mail: *rashedmehdi42@gmail.com*
[5] E-mail: *rishav16ban98@gmail.com*

2(a):

Caption of the following graph on page 50 will be replaced by:

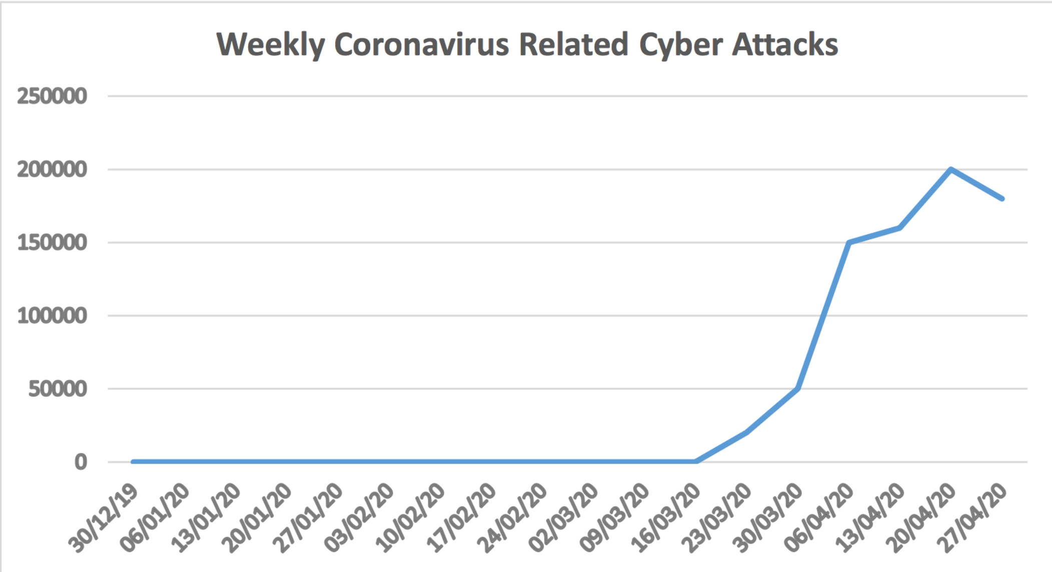

Graph showing the nature of increasing coronavirus themed cyber-attacks [7] (Source :ThreatCloud)

2(b):

Caption of the following graph on page 51 will be replaced by:

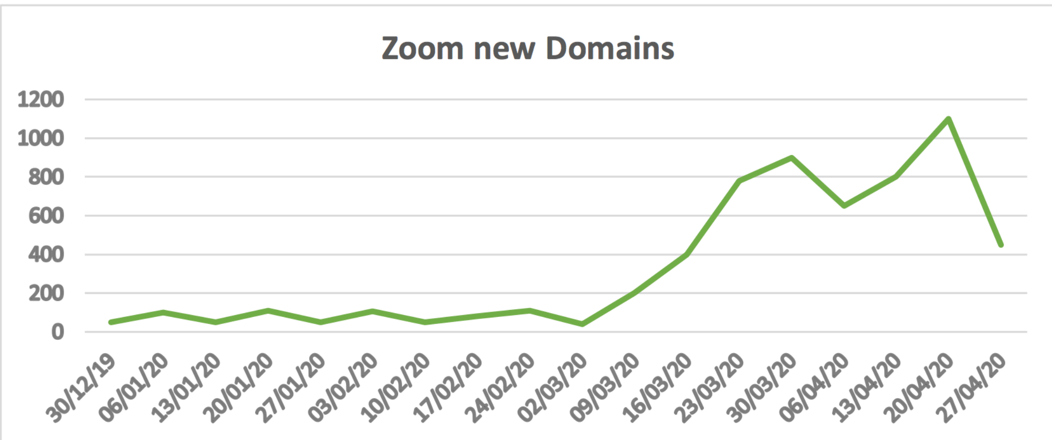

Graph showing the increasing frequency of registration of new Zoom domains themed on Coronavirus[7] (Source: ThreatCloud)